

## Updated analyses of temperature and precipitation extreme indices since the beginning of the twentieth century: The HadEX2 dataset

M. G. Donat,<sup>1</sup> L. V. Alexander,<sup>1,2</sup> H. Yang,<sup>1</sup> I. Durre,<sup>3</sup> R. Vose,<sup>3</sup> R. J. H. Dunn,<sup>4</sup> K. M. Willett,<sup>4</sup> E. Aguilar,<sup>5</sup> M. Brunet,<sup>5,21</sup> J. Caesar,<sup>4</sup> B. Hewitson,<sup>6</sup> C. Jack,<sup>6</sup> A. M. G. Klein Tank,<sup>7</sup> A. C. Kruger,<sup>8</sup> J. Marengo,<sup>9</sup> T. C. Peterson,<sup>3</sup> M. Renom,<sup>10</sup> C. Oria Rojas,<sup>11</sup> M. Rusticucci,<sup>12</sup> J. Salinger,<sup>13</sup> A. S. Elayah,<sup>14</sup> S. S. Sekele,<sup>8</sup> A. K. Srivastava,<sup>15</sup> B. Trewin,<sup>16</sup> C. Villarreal,<sup>17</sup> L. A. Vincent,<sup>18</sup> P. Zhai,<sup>19</sup> X. Zhang,<sup>18</sup> and S. Kitching<sup>2,20</sup>

Received 31 July 2012; revised 17 December 2012; accepted 27 December 2012; published 4 March 2013.

[1] In this study, we present the collation and analysis of the gridded land-based dataset of indices of temperature and precipitation extremes: HadEX2. Indices were calculated based on station data using a consistent approach recommended by the World Meteorological Organization (WMO) Expert Team on Climate Change Detection and Indices, resulting in the production of 17 temperature and 12 precipitation indices derived from daily maximum and minimum temperature and precipitation observations. High-quality in situ observations from over 7000 temperature and 11,000 precipitation meteorological stations across the globe were obtained to calculate the indices over the period of record available for each station. Monthly and annual indices were then interpolated onto a  $3.75^\circ \times 2.5^\circ$  longitude-latitude grid over the period 1901–2010. Linear trends in the gridded fields were computed and tested for statistical significance. Overall there was very good agreement with the previous HadEX dataset during the overlapping data period. Results showed widespread significant changes in temperature extremes consistent with warming, especially for those indices derived from daily minimum temperature over the whole 110 years of record but with stronger trends in more recent decades. Seasonal results showed significant warming in all seasons but more so in the colder months. Precipitation indices also showed widespread and significant trends, but the changes were much more spatially heterogeneous compared with temperature changes. However, results indicated more areas with significant increasing trends in extreme precipitation amounts, intensity, and frequency than areas with decreasing trends.

**Citation:** Donat, M. G., et al. (2013), Updated analyses of temperature and precipitation extreme indices since the beginning of the twentieth century: The HadEX2 dataset, *J. Geophys. Res. Atmos.*, 118, 2098–2118, doi:10.1002/jgrd.50150

<sup>1</sup>Climate Change Research Centre, University of New South Wales, Sydney, Australia.

<sup>2</sup>ARC Centre of Excellence for Climate System Science, University of New South Wales, Sydney, Australia.

<sup>3</sup>NOAA's National Climatic Data Center, Asheville, NC, USA.

<sup>4</sup>Hadley Centre, Met Office, Exeter, UK.

<sup>5</sup>Centre for Climate Change, Dep. Geography, Universitat Rovira i Virgili, Tarragona, Spain.

<sup>6</sup>Climate System Analysis Group, University of Cape Town, Cape Town, South Africa.

<sup>7</sup>Royal Netherlands Meteorological Institute (KNMI), De Bilt, Netherlands.

<sup>8</sup>Climate Service, South African Weather Service, Pretoria, South Africa.

<sup>9</sup>Earth System Science Centre (CCST), National Institute for Space Research (INPE), São Paulo, Brazil.

<sup>10</sup>Unidad de Ciencias de la Atmósfera, Universidad de la Republica, Montevideo, Uruguay.

<sup>11</sup>SENAMHI, Lima, Peru.

<sup>12</sup>Departamento de Ciencias de la Atmósfera y los Océanos, Universidad de Buenos Aires, Buenos Aires, Argentina.

<sup>13</sup>Woods Institute for the Environment, Stanford University, Stanford, CA, USA.

<sup>14</sup>Sudan Meteorological Authority (SMA), Khartoum, Sudan.

<sup>15</sup>India Meteorological Department, Pune, India.

<sup>16</sup>Bureau of Meteorology, Melbourne, Victoria, Australia.

<sup>17</sup>Oficina de Estudios, Direccion Meteorologica de Chile, Santiago, Chile.

<sup>18</sup>Climate Research Division, Environment Canada, Toronto, Canada.

<sup>19</sup>State Key Laboratory of Severe Weather, Chinese Academy of Meteorological Sciences, Beijing, China.

<sup>20</sup>Newcastle University, Newcastle upon Tyne, UK.

<sup>21</sup>Climatic Research Unit, School of Environmental Sciences, University of East Anglia, Norwich, UK.

Corresponding author: M. G. Donat, Climate Change Research Centre, University of New South Wales, Sydney, 2052, Australia. (m.donat@unsw.edu.au)

©2013. American Geophysical Union. All Rights Reserved.  
2169-897X/13/10.1002/jgrd.50150

## 1. Introduction

[2] The research into climate extremes has progressed enormously over the last few decades [Nicholls and Alexander, 2007; Zwiers *et al.*, 2012]. This has been largely due to international coordinated efforts to collate, quality control, and analyze variables and events that represent the more extreme aspects of climate. One such effort has been led by the Expert Team on Climate Change Detection and Indices (ETCCDI)<sup>1</sup> (<http://www.clivar.org/organization/etccdi>), who have facilitated the calculation of climate extremes indices based on daily temperature and precipitation data. This has been made possible through the provision of free standardized software for data analysis and quality control and through the organization of regional workshops to fill in data gaps in data-sparse regions [Peterson and Manton, 2008]. Unfortunately, the availability of daily observational high-quality data is limited for many regions of the globe. This is due to several reasons including a lack of suitable data but also because many countries have strict policies about data sharing. However, often National Meteorological Services are more willing to share derived indices, i.e., annual and/or monthly values derived from daily data that represent the number of days above or below a temperature or precipitation threshold for example. This helps to gain information about climate extremes from regions where daily data are not readily available to the scientific community. Thus, the development of the ETCCDI climate indices has enabled regional and global (both station and gridded) datasets to be developed [Zhang *et al.*, 2011] in a comparable way. One such global gridded dataset, HadEX, was developed by Alexander *et al.* [2006, henceforth A2006]. HadEX contains the 27 indices recommended by the ETCCDI (see Zhang *et al.* [2011] and [http://cccma.seos.uvic.ca/ETCCDI/list\\_27\\_indices.shtml](http://cccma.seos.uvic.ca/ETCCDI/list_27_indices.shtml)) on a  $3.75^\circ \times 2.5^\circ$  longitude-latitude grid from 1951 to 2003. In general, one index value was computed per grid box per year, although for some of the indices (e.g., hottest day/night, wettest day) seasonal values were also made available.

[3] HadEX currently represents the most comprehensive global gridded dataset of temperature and precipitation extremes based on daily in situ data available. It has been used in many model evaluation [e.g., Sillmann and Roekner, 2008; Alexander and Arblaster, 2009; Rusticucci *et al.*, 2010; Sillmann *et al.*, 2011] and detection and attribution studies [e.g., Min *et al.*, 2012; Morak *et al.*, 2011], in addition to climate variability and trend studies (e.g., A2006). Nonetheless, it covers a relatively short period (53 years) and contains numerous data gaps both in space and time, and this is particularly the case for the precipitation indices.

[4] The purpose of the current study is to update HadEX to develop the HadEX2 dataset and to document and assess this new dataset. This new version of the dataset contains many more input station data than the earlier version of the dataset and covers a much longer period, 1901 to 2010. In the next sections, we describe the data and indices used as

input to HadEX2, the gridding method used to develop grids of the different extremes indices, and the analysis of this dataset over global land areas.

## 2. Data and Indices

[5] All of the climate indices are calculated from daily observations of precipitation, maximum temperature, and minimum temperature. The indices calculated for HadEX2 are shown in Table 1. These mostly represent the indices recommended by the ETCCDI (see <http://cccma.seos.uvic.ca/ETCCDI/indices.shtml>), although one of the recommended 27 indices is user-defined (Rnnmm: annual count of precipitation above a user-chosen threshold) and is therefore excluded, and three additional indices are included: Extreme Temperature Range (ETR), contribution from very wet days (R95pTOT), and contribution from extremely wet days (R99pTOT), as these were also included in HadEX due to their potential to have significant societal impacts. A total of 29 indices are therefore calculated. The original station network used in HadEX contained 2223 temperature and 5948 precipitation stations (see Fig. 1 of A2006). The total number of stations available for HadEX2 is generally about twice that available for HadEX (see Table 1) and includes improved spatial coverage of stations in southern Africa, South America, Southeast Asia, and Australasia. The (monthly) index values were calculated only if fewer than three daily observations were missing in a month and accordingly fewer than 15 daily observations per year for the annual indices. If more daily observations were missing, the climate index was set to a missing value for that specific month or year. The annual index values were also set to missing if one of the months was assigned a missing value.

[6] The spatial coverage of stations varies among indices, and there are many more stations containing precipitation than temperature data. It is generally necessary to have a larger number of representative precipitation stations since the spatial variability of precipitation extremes is much higher than for temperature extremes [Kiktev *et al.*, 2003; A2006]. Figures 1a and 1c show the spatial coverage of stations for an example temperature (TXx) and precipitation (Rx1day) index. The color coding in the maps in Figure 1 indicates the data source. The largest number of stations was obtained from international data initiatives including the following:

[7] 1. The European Climate Assessment and Dataset (ECA&D) [Klok and Klein Tank, 2009], containing approximately 6600 stations from 62 countries across Europe and North Africa

[8] 2. The Southeast Asian Climate Assessment and Dataset (SACAD)—as ECA&D but currently containing more than 1000 stations from 11 countries across Southeast Asia (we removed the Australian stations from this data set, as a separate data set of high-quality stations was used for Australia; see Table 2)

[9] 3. The Latin American Climate Assessment and Dataset (LACAD)—as ECA&D but currently containing about 300 stations from seven countries across Latin America

[10] 4. The Global Historical Climatology Network-Daily (GHCN-Daily) [Menne *et al.*, 2012]. Comprising approximately 27,000 stations globally with daily maximum and

<sup>1</sup>Joint World Meteorological Organization (WMO) Commission for Climatology (CCI)/World Climate Research Programme (WCRP) project on Climate Variability and Predictability (CLIVAR)/Joint WMO-Intergovernmental Oceanographic Commission of the United Nations Educational, Scientific and Cultural Organization (UNESCO) Technical Commission for Oceanography and Marine Meteorology (JCOMM) Expert Team on Climate Change Detection and Indices.

**Table 1.** The Extreme Temperature and Precipitation Indices Available in HadEX2 along with the Number of Stations That Was Included for Each Index<sup>a</sup>

ID	Indicator Name	Indicator Definitions	Number of	
			Units	Stations
<b>TXx</b>	Hottest day	Monthly maximum value of daily max temperature	°C	7381
<b>TNx</b>	Warmest night	Monthly maximum value of daily min temperature	°C	7390
<b>TXn</b>	Coldest day	Monthly minimum value of daily max temperature	°C	7381
<b>TNn</b>	Coldest night	Monthly minimum value of daily min temperature	°C	7390
<b>TN10p</b>	Cool nights	Percentage of time when daily min temperature < 10 <sup>th</sup> percentile	%	6619
<b>TX10p</b>	Cool days	Percentage of time when daily max temperature < 10 <sup>th</sup> percentile	%	6619
<b>TN90p</b>	Warm nights	Percentage of time when daily min temperature > 90 <sup>th</sup> percentile	%	6617
<b>TX90p</b>	Warm days	Percentage of time when daily max temperature > 90 <sup>th</sup> percentile	%	6598
<b>DTR</b>	Diurnal temperature range	Monthly mean difference between daily max and min temperature	°C	7365
GSL	Growing season length	Annual (1st Jan to 31st Dec in NH, 1st July to 30th June in SH) count between first span of at least 6 days with TG > 5°C and first span after July 1 (January 1 in SH) of 6 days with TG < 5°C (where TG is daily mean temperature)	days	6843
ID	Ice days	Annual count when daily maximum temperature < 0°C	days	7120
FD	Frost days	Annual count when daily minimum temperature < 0°C	days	7150
SU	Summer days	Annual count when daily max temperature > 25°C	days	7168
TR	Tropical nights	Annual count when daily min temperature > 20°C	days	7179
WSDI	Warm spell duration index	Annual count when at least six consecutive days of max temperature > 90 <sup>th</sup> percentile	days	6600
CSDI	Cold spell duration index	Annual count when at least six consecutive days of min temperature < 10 <sup>th</sup> percentile	days	6594
<b>Rx1day</b>	Max 1 day precipitation amount	Monthly maximum 1 day precipitation	mm	11588
<b>Rx5day</b>	Max 5 day precipitation amount	Monthly maximum consecutive 5 day precipitation	mm	11607
SDII	Simple daily intensity index	The ratio of annual total precipitation to the number of wet days (≥ 1 mm)	mm/day	11607
R10mm	Number of heavy precipitation days	Annual count when precipitation ≥ 10 mm	days	11607
R20mm	Number of very heavy precipitation days	Annual count when precipitation ≥ 20 mm	days	11588
CDD	Consecutive dry days	Maximum number of consecutive days when precipitation < 1 mm	days	11602
CWD	Consecutive wet days	Maximum number of consecutive days when precipitation ≥ 1 mm	days	11583
R95p	Very wet days	Annual total precipitation from days > 95 <sup>th</sup> percentile	mm	11580
R99p	Extremely wet days	Annual total precipitation from days > 99 <sup>th</sup> percentile	mm	11580
PRCPTOT	Annual total wet day precipitation	Annual total precipitation from days ≥ 1 mm	mm	11588
<b>*ETR</b>	Extreme temperature range	TXx – TNn	°C	7159
<b>*R95pTOT</b>	Contribution from very wet days	100 * R95p / PRCPTOT	%	11300
<b>*R99pTOT</b>	Contribution from extremely wet days	100 * R99p / PRCPTOT	%	11300

<sup>a</sup>Most indices are recommended by the Expert Team on Climate Change Detection and Indices (ETCCDI) (see [http://cccma.seos.uvic.ca/ETCCDI/list\\_27\\_indices.html](http://cccma.seos.uvic.ca/ETCCDI/list_27_indices.html)) except those marked with an asterisk. Indices in bold represent those that are also available monthly.

minimum temperature and over 80,000 stations with daily precipitation amounts, GHCN-Daily however is used only in this study for a subset of stations in the U.S. Although subjected to a comprehensive set of quality assurance procedures [Durre *et al.*, 2010], GHCN-Daily data are not adjusted for artificial discontinuities such as those associated with changes in observation time, instrumentation, and station location. To circumvent this, the subset chosen for the U.S. followed the analysis by Peterson *et al.* [2008], who only selected National Weather Service Cooperative and First-Order weather observing sites with reasonably long records. Data were used only from station time series that were determined (e.g., by the statistical analysis described in Menne and Williams [2005]) to be free of significant discontinuities after 1950 caused by changes in station location, changes in time of observation, etc.

[11] Other stations used in this study have been supplied by the authors either through their personal research or from the National Meteorological Service in that country. For all regions, at least one of the authors had access to the daily data from which the indices were calculated. Therefore reference could always be made to the original data should quality issues arise during the analysis (see Table 2). Additional stations were obtained through ETCCDI regional workshops, although in a small number of cases the raw data were not available and only the derived indices were provided.

[12] While the level of quality control varies from country to country, in most cases the data have been carefully assessed for quality and homogeneity by researchers in the country of origin. For example, Canada supplied homogenized daily temperatures up to 2010 for 338 stations [Vincent *et al.*, 2012] and a high-quality adjusted precipitation data set for 464 stations [Mekis and Vincent, 2011]. Australian temperature records were updated from those used in HadEX, adjusting for inhomogeneities at the daily timescale by taking account of the magnitude of discontinuities for different parts of the distribution, increasing the number of stations available to 112 and extending the record back in time to 1910 [Trewin, 2012]. Indian data have only been used from India Meteorological Department (IMD) observatory stations where exposure conditions have remained the same and meteorological instruments are maintained as per WMO guidelines. In Argentina and Uruguay, stations with known inhomogeneities or long periods without data were excluded from the index calculation. In the case of the ETCCDI workshop data, extensive postprocessing and analysis was performed [e.g., Aguilar *et al.*, 2009; Caesar *et al.*, 2011; Vincent *et al.*, 2011] to ensure data quality and homogeneity. Note therefore that because of the updates to high-quality station availability for many regions, HadEX2 provides not just an extension of

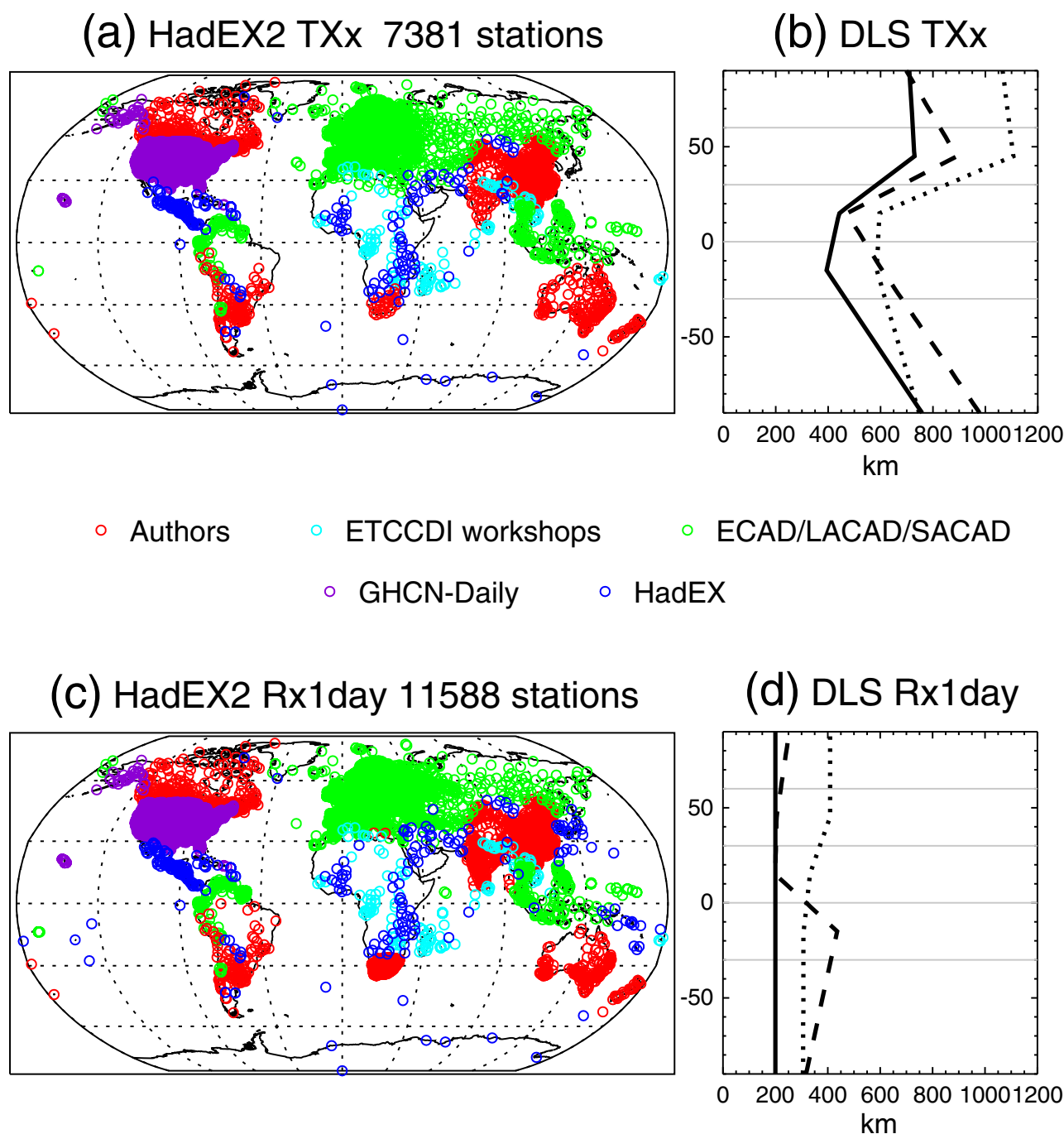


**Figure 1.** Maps indicate locations of stations used in HadEX2 for an example temperature and precipitation index. (a) TXx and (c) Rx1day. Sources of data (see text) are color coded. (b and d) The decorrelation length scales (in km) for each latitude band for TXx and Rx1day, respectively for annual (solid line), January (dotted line), and July (dashed line). Thin gray lines indicate the borders of latitude bands used for grouping the stations when calculating the decorrelation length scales (see text for details).

stations used in HadEX but rather represents the latest acquisition of high-quality station data around the globe.

[13] Table 2 indicates the sources of all the data used in this study, and relevant references where applicable. However, since the spatial coverage deteriorated in some cases between HadEX and HadEX2, particularly for Africa and parts of South and Central America, the station coverage

was supplemented using existing stations from HadEX where there were no stations in HadEX2 within a 200 km radius of a HadEX station. This provided about an additional 200 stations for temperature indices and 280 stations for precipitation indices. While the addition of HadEX stations offers some improvement in coverage, data included in HadEX2 are still sparse at the beginning and end of the



**Table 2.** References and Contacts for Data Used to Create HadEX2<sup>a</sup>

Source Region/Dataset	Contact	Reference(s) if available
Arab region workshop	Paper author: m.donat@unsw.edu.au	<i>Donat et al.</i> [2012b]
Argentina	Paper author: mati@at.fcen.uba.ar	<i>Rusticucci</i> [2012]
Australia	Paper author: b.trewin@bom.gov.au	<i>Trewin</i> [2012]
Brazil	http://www.inmet.gov.br, Paper author: jose.marengo@inpe.br	
Canada	Paper authors: Lucie.Vincent@ec.gc.ca (for temperature); Eva.Mekis@ec.gc.ca (for precipitation)	<i>Mekis and Vincent</i> [2011]; <i>Vincent et al.</i> [2012]
Chile	Paper author: cvilla@meteochile.com	<i>Villarroel et al.</i> [2006]
China	Chinese Meteorological Administration (CMA)	<i>Zhai et al.</i> [2005]; <i>Zhai and Pan</i> [2003]
Congo workshop	Paper authors: enric.aguilar@urv.cat; Xuebin.zhang@ec.gc.ca; manola.brunet@urv.cat	<i>Aguilar et al.</i> [2009]
ECAD	The European Climate Assessment and Dataset: <a href="http://eca.knmi.nl/">http://eca.knmi.nl/</a>	<i>Klok and Klein Tank</i> [2009]
HadEX	Climdex project: <a href="http://www.climdex.org">http://www.climdex.org</a>	<i>Alexander et al.</i> [2006]
India	Paper author: aks_ncc2004@yahoo.co.in	
Latin America	Latin American Climate Assessment and Dataset: <a href="http://lacad.ciifen-int.org/download/millennium/millennium.php">http://lacad.ciifen-int.org/download/millennium/millennium.php</a>	
New Zealand	Paper author: salinger@stanford.edu	<i>Griffiths et al.</i> [2003], <i>Salinger and Griffiths</i> [2001]
Peru	Paper author: clara@senamhi.gob.pe	<i>Oria</i> [2012]
South Africa	Paper authors: hewitson@csag.uct.ac.za; Andries.Kruger@ weathersa.co.za; cjack@csag.uct.ac.za	<i>Kruger and Sekele</i> [2012]
Southeast Asia	Southeast Asian Climate Assessment and Dataset: <a href="http://saca-bmkg.knmi.nl/">http://saca-bmkg.knmi.nl/</a>	
Uruguay	Paper author: renom@fisica.edu.uy	<i>Rusticucci and Renom</i> [2008]
USA	Global Historical Climatology Network - Daily: <a href="http://www.ncdc.noaa.gov/oa/climate/ghcn-daily/">http://www.ncdc.noaa.gov/oa/climate/ghcn-daily/</a>	<i>Durre et al.</i> [2010]; <i>Menne et al.</i> [2012]; <i>Peterson et al.</i> [2008]
Vietnam workshop	Paper author: john.caesar@metoffice.gov.uk	<i>Caesar et al.</i> [2011]
West Indian Ocean workshop	Paper author: Lucie.Vincent@ec.gc.ca	<i>Vincent et al.</i> [2011]

<sup>a</sup>In most cases, the indices were calculated by the contact author and sent to the lead author for inclusion in HadEX2.

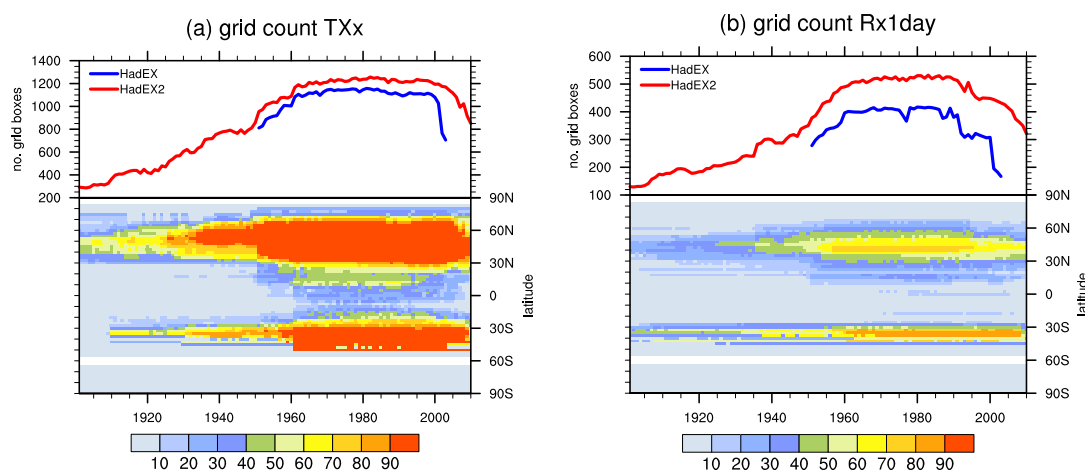


**Figure 2.** Time series of annual grid box coverage (out of a total of 2382 land grids for the chosen longitude-latitude grid) for (a) TXx and (b) Rx1day from 1901 to 2010 for HadEX2 and 1951 to 2003 for HadEX (A2006) after gridding (see text for details). Top panel shows the total number of grid boxes with nonmissing data globally; bottom panel shows the percentage of land grid boxes with nonmissing data at each latitude.

record in addition to some stations only having short records. Particularly in the most recent years since 2006, there is a decrease in the number of available observational data, which also leads to a strong decline in spatial coverage of HadEX2 during the last 5 years (Figure 2). Data for both temperature and precipitation prior to 1950 are mostly confined to Eurasia, North America, Southern South America, Australasia, and India (precipitation only).

[14] To ensure consistency in the calculation of indices among regions, the RCLimDex/FClimDex software packages were used (see *Zhang et al.* [2011] and <http://ccma.seos.>

[uvic.ca/ETCCDI/software.shtml](http://uvic.ca/ETCCDI/software.shtml)). Percentiles required for some of the temperature indices (Table 1) were calculated for the climatological base period 1961–1990 using a bootstrapping method proposed by *Zhang et al.* [2005]. The bootstrapping approach is intended to eliminate possible inhomogeneities at the boundaries of the climatological base period due to sampling error. The percentiles are calculated only if at least 75% of nonmissing daily temperatures are available during the base period. In addition, problems with data precision have arisen in some countries such as rounding to whole degrees in recording, and this can also affect

trend estimates for some indices [Zhang *et al.*, 2009]. This has been accounted for by adding a small random number to improve the granularity of data and thus making the estimation of the threshold more accurate [Zhang *et al.*, 2009; Zhang *et al.*, 2011].

[15] Note, however, that the data for ECA&D, SACAD, and LACAD were processed slightly differently. These groups calculate many more indices than those recommended by ETCCDI, but the output from these datasets is processed in such a way as to be comparable with the output from RClimDex/FClimDex for the ETCCDI indices. One exception is the calculation of very wet days (R95p) and extremely wet days (R99p). While these indices commonly refer to the precipitation amount above the respective percentile value, ECA&D, SACAD, and LACAD instead counted the number of days when the percentile is exceeded. For this analysis, we therefore recalculated their data for these two indices from the calculated values of R95pTOT and PRCPTOT (i.e.,  $R95pTOT \times PRCPTOT / 100$ ), so that they matched the index definition proposed by the ETCCDI, and in turn providing a consistent analysis approach for all regions. During this process, we discovered some inconsistencies in a handful of the SACAD stations which affected the calculation of indices that required a climatological percentile to be calculated, e.g., in some instances the annual value for R99p was the same as PRCPTOT. This resulted in the removal of five stations in Malaysia and three stations in Indonesia.

### 3. Gridding Method

[16] Our gridding method closely follows that of HadEX (see Appendix A of A2006 for details of the gridding procedure) with only some very minor differences. Climate indices are calculated for each station and then interpolated onto a regular grid, using a modified version of Shepard's angular distance weighting (ADW) interpolation algorithm [Shepard, 1968]. The ADW gridding algorithm has been used by a number of studies for gridding similar data sets of climate extremes [Kiktev *et al.*, 2003; A2006], daily temperatures [Caesar *et al.*, 2006], or monthly climate variables [New *et al.*, 2000] and has generally been shown to be a good method when gridding irregularly spaced data. Gridding the observations helps to solve several issues, including uneven station distribution when calculating global averages [Frich *et al.*, 2002], and to minimize the impact of data quality issues at individual stations due to averaging.

[17] The ADW interpolation method requires knowledge of the spatial correlation structure of the station data. We assume that station pairings greater than 2000 km apart or stations with short overlapping data will not provide meaningful correlation information. Therefore, correlations between all station pairs within a 2000 km radius are calculated if there are overlapping data for at least a 30 year period. Correlations are performed on all available data after 1951, the period when most of the stations used in this study have good temporal coverage. However, the correlation results are almost identical even if the period is extended back to 1901 (where suitable station pairings are available). In order that we can compare HadEX2 results with those from HadEX, the method of A2006 is followed such that the interstation correlations are then averaged into 100 km bins, and a second-order polynomial function is fitted to the resulting

data assuming that correlations equal 1 at 0 distance. The decorrelation length scale (DLS) is defined as the distance at which the correlation function falls below  $1/\exp(1)$  and represents the maximum “search radius” in which station data are considered for the calculation of grid point values. In addition, the polynomial function is tested to determine whether it is a good fit to the data at the 5% significance level using a chi-square statistic (for an example of this type of function, see Fig. A1 of A2006). If the function is found not to be a good fit, then the decorrelation length scale is set to 200 km, the minimum value set for search radius distance. This differs slightly from HadEX where the minimum DLS was set to 100 km, but it was decided for HadEX2 that this minimum value should be more reflective of the size of the grid boxes that were being used. Note that this scale does not necessarily reflect the observed spatial variability of precipitation. However, for most indices and latitude bands, the DLS was found to be greater than 200 km. Only for the annual Rx1day, R99p, and CWD (see Table 1) indices is the minimum DLS calculated at a number of latitudes (e.g., Figure 1d).

[18] Decorrelation length scale values are calculated for each index separately. As in HadEX, DLS values are calculated independently for four non-overlapping 30°-latitude zonal bands between 90°N and 30°S, plus a 60° band spanning the data-sparse 30° to 90°S latitudes (the reasons for this are described in Appendix A of A2006 but include a compromise between data density and actual covariability of indices and the reasoning that temperature variations in particular are more coherent zonally rather than meridionally). For indices with monthly output, the DLS is calculated for both the monthly and annual index values. Linear interpolation is used to smooth the DLS values between bands and avoid discontinuities at the band boundaries. For comparison with HadEX, we chose the same  $3.75^\circ \times 2.5^\circ$  longitude-latitude grid, resulting in a separate DLS value for each  $2.5^\circ$  latitude band. Examples of the DLS values are given in Figures 1b and 1d. The interstation correlations and thus the DLS are, unsurprisingly, generally larger for the temperature-based indices than for the precipitation extremes and for monthly rather than annual values.

[19] Grid box values are calculated based on all station data within the DLS and weighted according to their distance from the grid box center using a modified version of Shepard's ADW interpolation algorithm (see equation A2 of Appendix A in A2006). A minimum of three stations are required to be within the DLS before a grid box value can be calculated; otherwise a missing data value is assigned. The weight decays exponentially with increasing distance, but additional information relating to the angle of the locations of the stations to each grid box center is also included to account for how bunched or isolated the stations are within the search radius. An additional parameter adjusts the steepness of the decay [Caesar *et al.*, 2006; A2006]. Again for consistency with HadEX, we set this parameter equal to 4, as this was found to provide a reasonable compromise between reducing the root mean squared error (RMSE) between gridded and station data and spatial smoothing. However, for global, continental, and even regional averages, the results are almost identical when using values between 1 and 10 for this parameter.

[20] Besides updating HadEX for the most recent years, we also extended the gridded product, although with limited coverage, back to the first half of the twentieth century, calculating grids over the period 1901 to 2010. In the next section, we present trends for two periods: 1951–2010 and 1901–2010. Trends are calculated for each grid box assuming that index values for the grid box are available for at least 66% of the years (i.e., 40 years out of 1951–2010 and 73 years out of the 1901–2010 period) and that data are available through at least 2003. In order to avoid the spurious influence of varying spatial coverage, global time series of area-weighted averages are calculated using only grid boxes that have at least 90% of data during the periods presented (i.e., 54 years out of the 1951–2010 period and 99 years out of the 1901–2010 period). Note that, owing to limited spatial coverage, the “global time series” are not representative for the entire globe and rather should be interpreted as “area averages of all sufficiently covered regions.” Particularly for the 110 year period 1901–2010, the 90% completeness criterion restricts the grid boxes contributing to the “global time series” to grid boxes from North America, Eurasia, Australia, parts of southern South America, and India (precipitation only). The trends presented here (Figures 3 to 9) are calculated using Sen’s trend estimator [Sen, 1968], and trend significance is estimated at the 5% level using the Mann-Kendall test [Kendall, 1975]. This method was chosen because it makes no assumptions about the distribution of the variable and some of the climate indices do not follow a Gaussian distribution. Note that while linear trends are widely used and an easily understandable measure for documenting changes in climate indices, they are not necessarily the best fit to the observed changes presented here. Therefore, we supplement our global time series plots by also showing 21 year smoothed functions to represent some of the decadal variations that have been observed since the beginning of the twentieth century.

## 4. Results

[21] Trends (shown as maps) are presented using data for each index for 110 years since 1901 and for 60 years since 1951, when spatial coverage is more complete and other observational data sets begin [e.g., Caesar *et al.*, 2006; Donat *et al.*, 2012a; A2006]. Hatching in Figures 3–9 indicates regions where trends are significant at the 5% level.

[22] While trend maps can obviously highlight regional detail, the focus of this paper is to assess broad scale changes in extremes. We therefore mostly limit our discussion of results to an assessment of global change, while we acknowledge that regional studies can provide much more in-depth analysis, although we do draw attention to interesting or unusual regional detail.

### 4.1. Trends in Annual Temperature Indices

[23] All temperature-related indices show significant and widespread warming trends, which are generally stronger for indices calculated from daily minimum (nighttime) temperature than for those calculated from daily maximum (daytime) temperature.

[24] For example, the frequency of cool nights based on daily minimum temperatures is shown to have significantly decreased almost everywhere during the past 60 years (Figure 3a). The strongest reductions, up to 3 days per

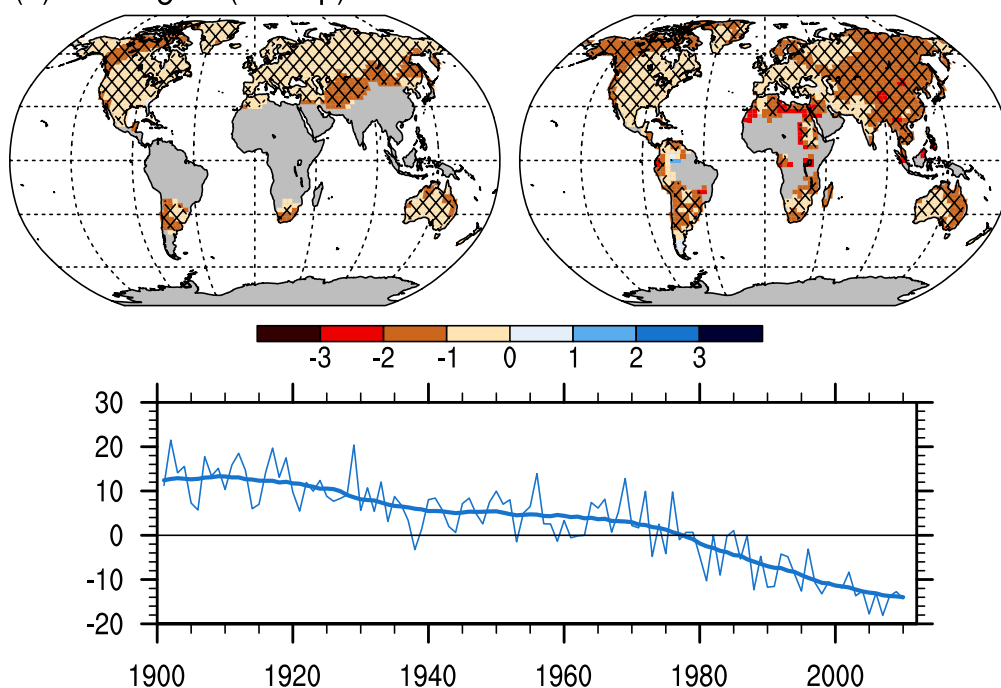
decade since 1951 are found over eastern Asia, northern Africa, and in some regions of South America (the average annual frequency during the 1961–1990 base period is by definition 36.5 days). Globally averaged, the frequency of cool nights has decreased by about 50% (18 days) between the 1950s and the first decade of the 21st century. Correspondingly, at the upper tail of the minimum temperature distribution, we find a significant increase in the frequency of warm nights in almost all regions (Figure 3c). Globally averaged, the frequency of warm nights has increased by about 55% (20 days in a year) during the past 60 years. Of the grid boxes with valid data, 98% show significant ( $p \leq 0.05$ ) increases in TN90p and decreases in TN10p, respectively (Table 3).

[25] Analyzing daytime temperature extremes, we see a reduction in the number of cool days and an increased frequency of warm days (Figures 3b and 3d). The changes in cool and warm days appear to be somewhat smaller compared to the cool and warm night frequency changes. The trends are also spatially less homogeneous in sign, as slight cooling trends are found over eastern North America (the so-called “warming hole,” Portmann *et al.* [2009]) and along the South-American west coast areas (in particular the northern part of Chile). Still, in most regions and in the global average, there are significant warming trends resulting in less frequent cool and more frequent warm days. In addition, 77 (84)% of the global land area covered by HadEX2 shows a significant increase in warm days (decrease in cool days) (see Table 3).

[26] Mostly warming trends are also apparent in the absolute warmest and coldest temperatures of the year. The warming is generally stronger for the coldest than for the warmest value. Since the middle of the twentieth century, the coldest night (TNn) and coldest day (TXn) of the year, for example, have significantly increased over much of Asia, North America, Australia, and southern South America (Figures 4a and 4b). Warming trends are particularly strong (up to 1°C per decade) over large parts of Asia. Seventy percent (52%) of the grid boxes with sufficient data coverage show significant increases in TNn (TXn) during the 1951 to 2010 period, whereas significant decreases are only found in 3% (4%) of the grid boxes (Table 3). Globally averaged, the temperature related to the coldest night of the year (TNn) has increased by about 3°C in the past 60 years.

[27] Warming (but mostly weaker) trends are also found for temperatures related to the warmest night (TNx) and the warmest day (TXx) over much of Europe, Asia, and northeastern North America, whereas a significant decrease in TXx is found over the eastern U.S. and in South America over parts of Argentina and Uruguay (Figures 4c and 4d). On average globally, both TNx and TXx have increased by about 1°C since the 1950s; however, for TXx similarly high values as today seem to have also occurred in the 1930s. Particularly high annual maximum temperatures (TXx) occurred, e.g., over North America in the 1930s. Sixty-four percent (32%) of grid boxes show significant increases in TNx (TXx), as opposed to 3% (6%) with significant decreases. Over most regions, the increases in TNn are stronger than increases in TXx. Consequently, the extreme temperature range (ETR) is reduced, in particular over North America, Asia, and South America and also on the global average (not shown).

## (a) cool nights (TN10p)



## (b) cool days (TX10p)

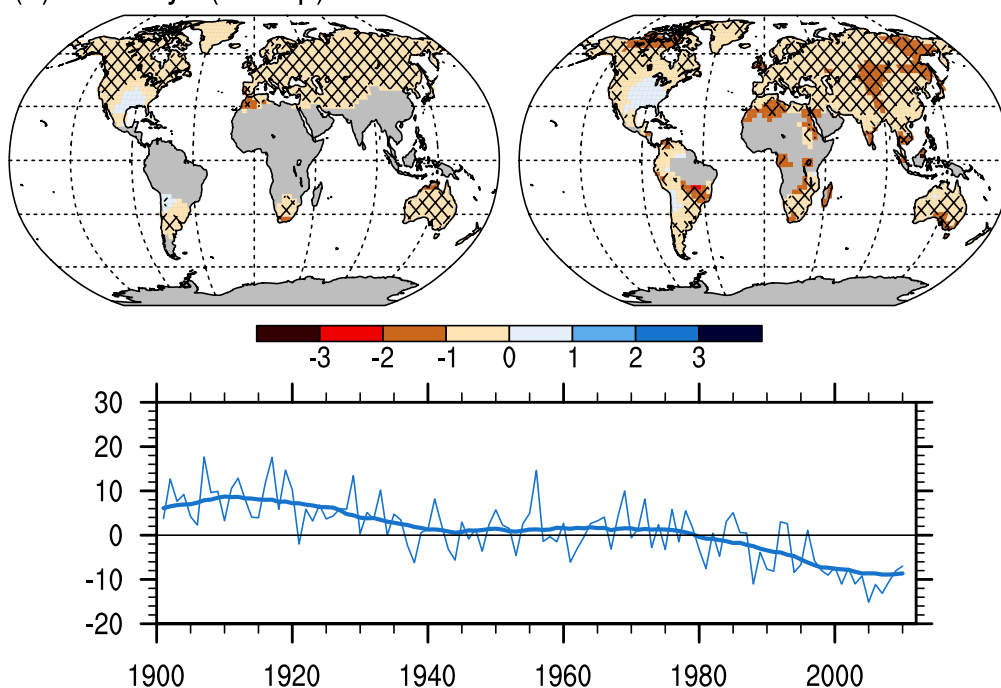
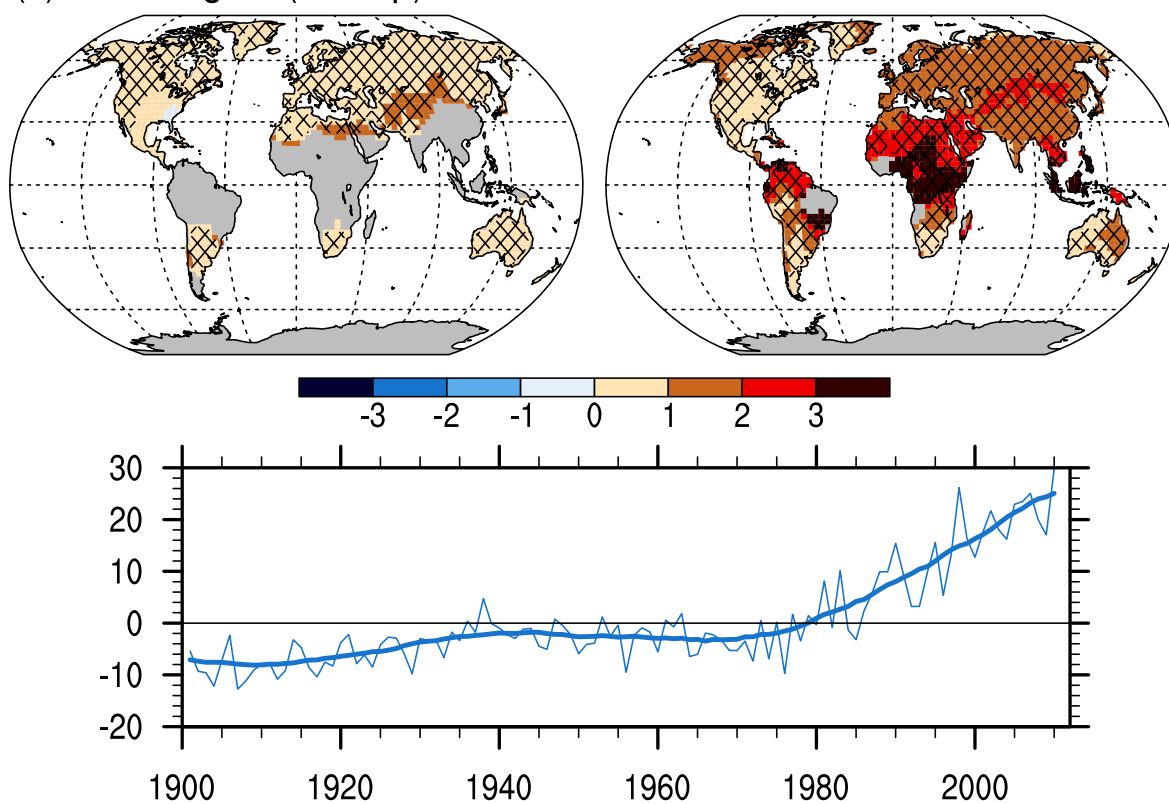


**Figure 3.** Trends (in annual days per decade, shown as maps) for annual series of percentile temperature indices for (left) 1901–2010 and (right) 1951–2010 for (a) cool nights (TN10p), (b) warm nights (TN90p), (c) cool days (TX10p), and (d) warm days (TX90p). Trends were calculated only for grid boxes with sufficient data (at least 66% of years having data during the period, and the last year of the series is no earlier than 2003). Hatching indicates regions where trends are significant at the 5% level. The time series show the global average annual values (in days per year) for the same indices as anomalies relative to 1961–1990 mean values (thin blue line). The thick blue line shows the 21 point Gaussian filtered data for HadEX2. Note that for the global average time series only grid boxes with at least 90% of temporal coverage are used, i.e., 99 years during 1901–2010 (see text). Note that in this figure the units were converted to days per year prior to calculation.



## (c) warm nights (TN90p)



## (d) warm days (TX90p)

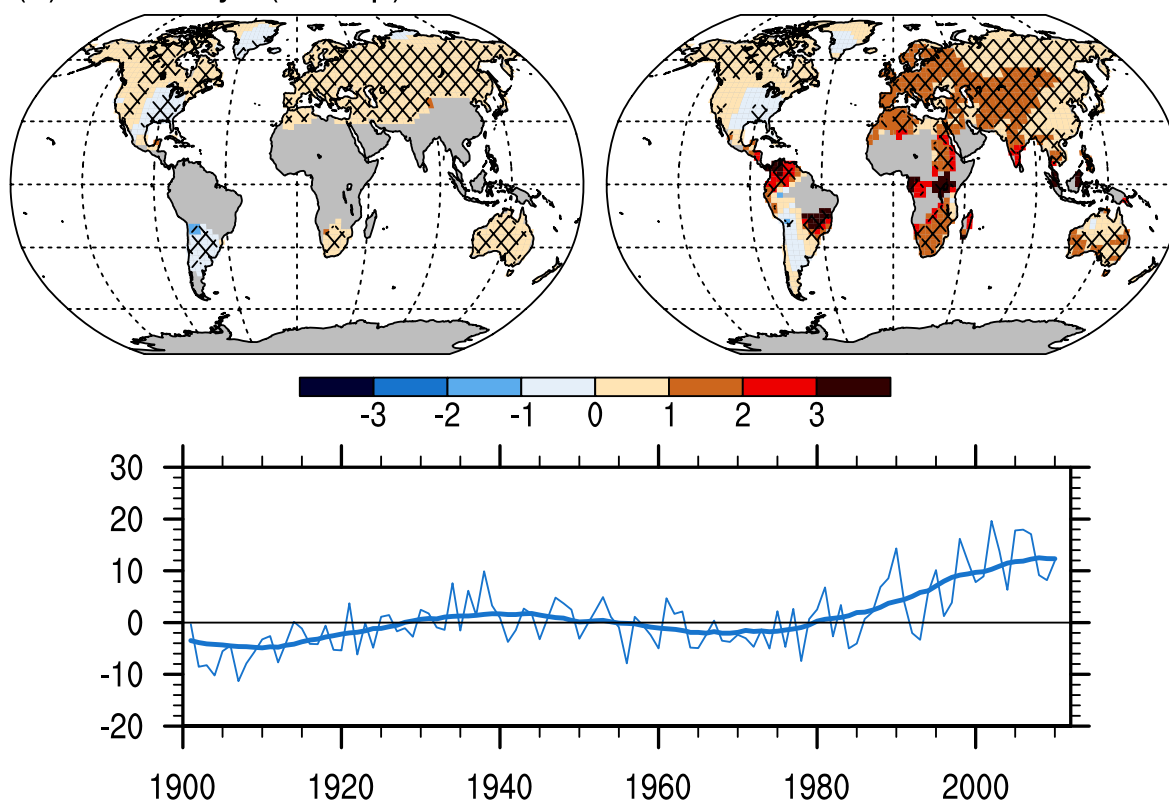
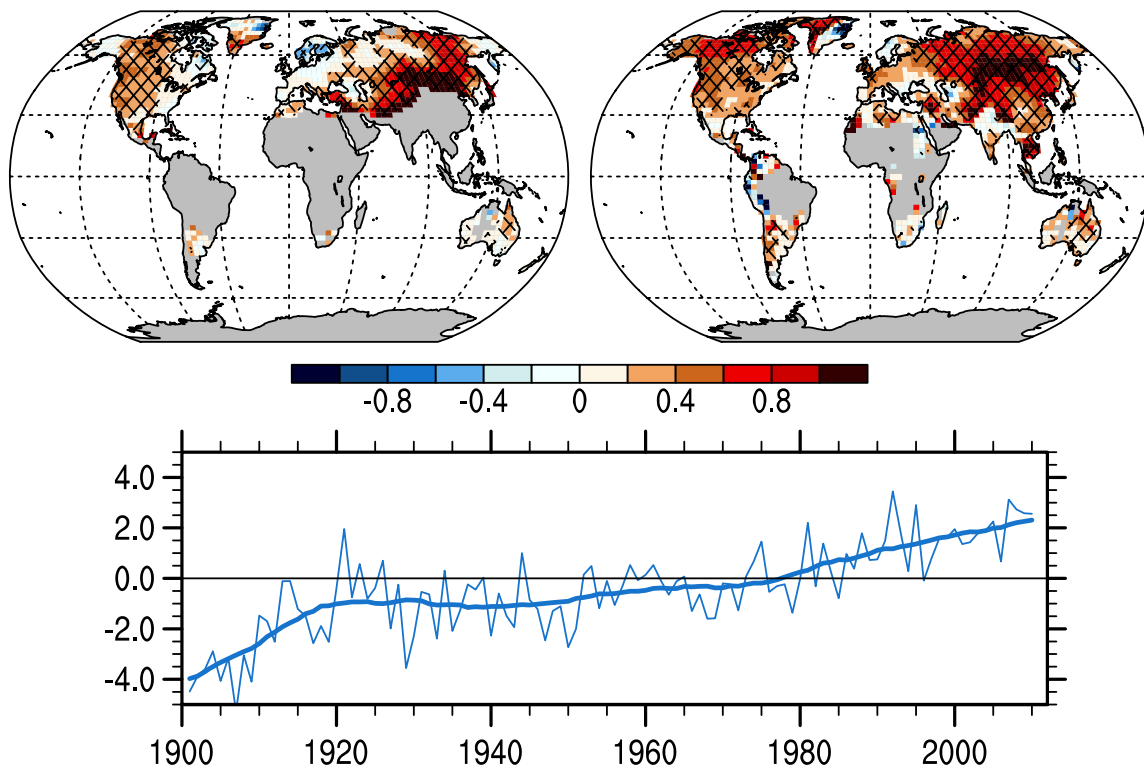
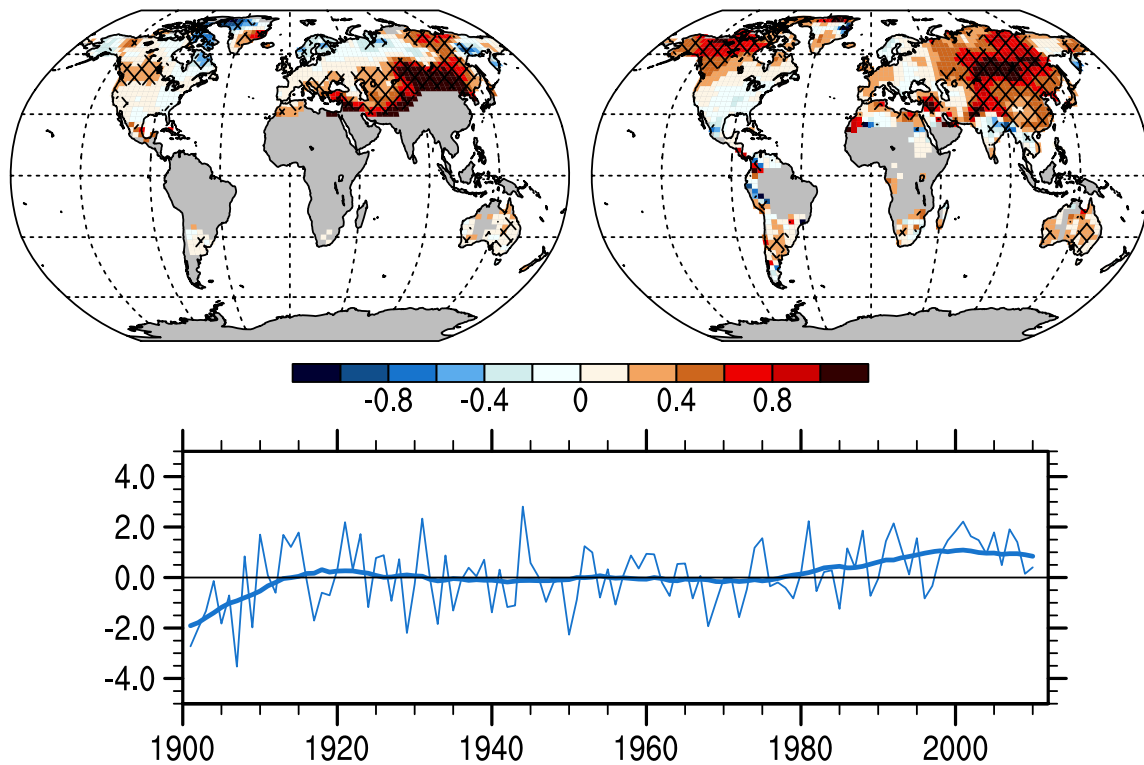


Figure 3. (Continued)

## (a) coldest night (TNn)

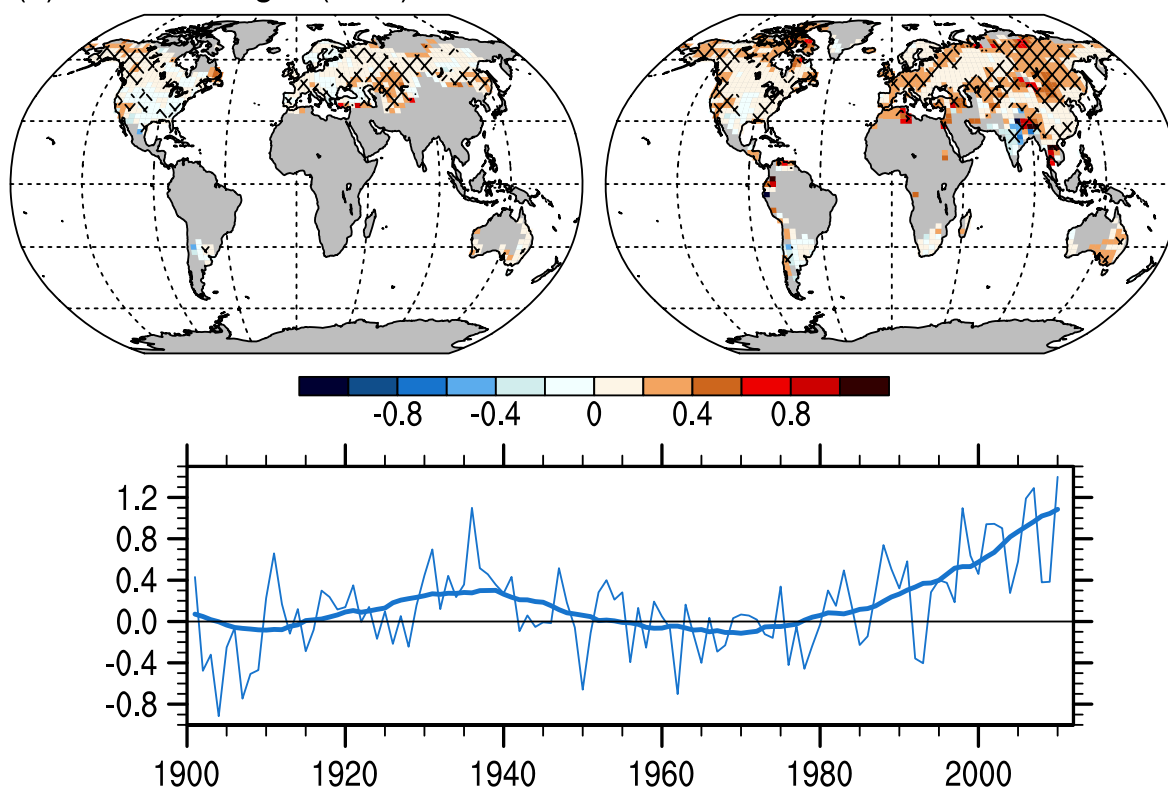


## (b) coldest day (TXn)



**Figure 4.** Trend maps and global average time series for annual indices, (a) coldest night (TNn) in °C, (b) coldest day (TXn) in °C, (c) warmest night (TNx) in °C, and (d) hottest day (TXx) in °C. Details of trend and time series calculations as described in Figure 3.

## (c) warmest night (TNx)



## (d) hottest day (TXx)

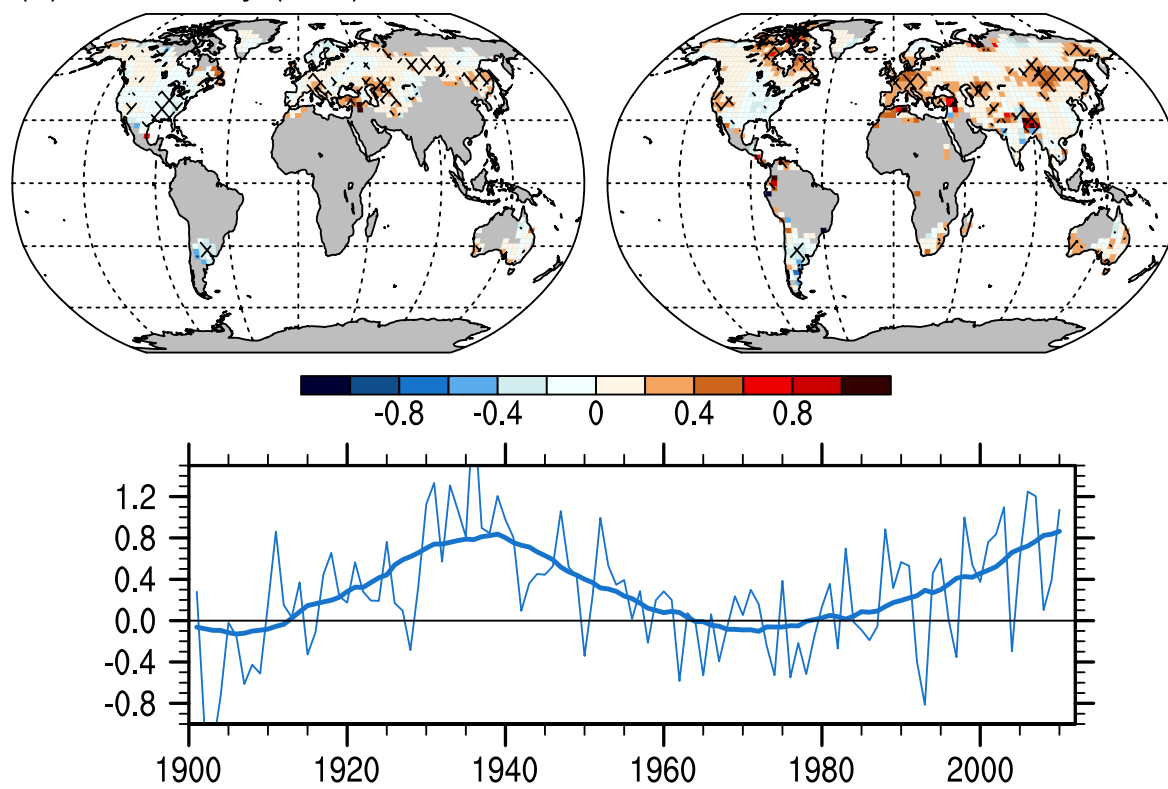
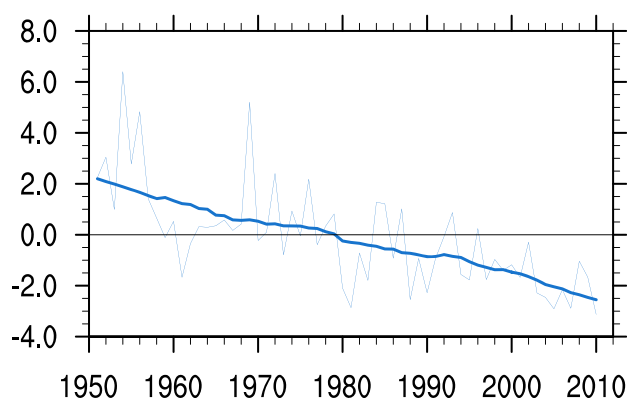
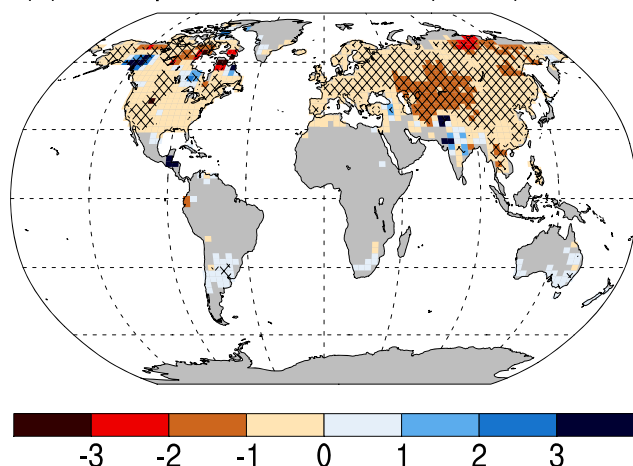
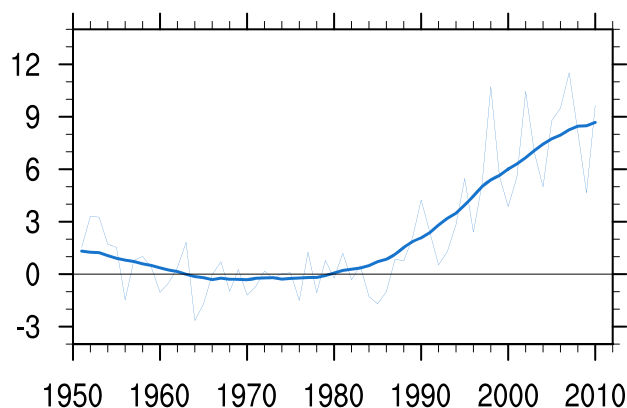
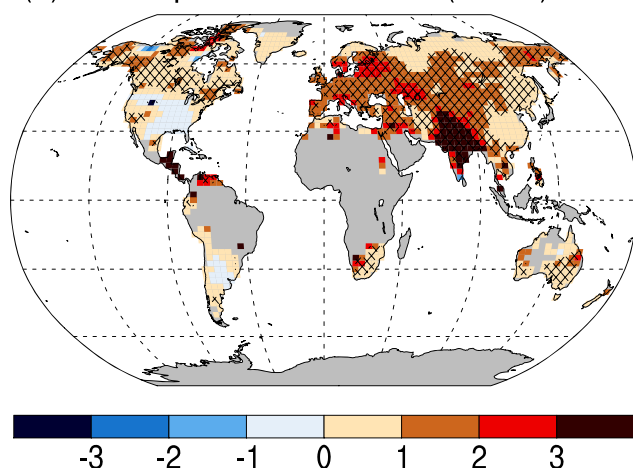


Figure 4. (Continued)

## (a) cold spell duration index (CSDI)



## (b) warm spell duration index (WSDI)



**Figure 5.** Trends (in annual days per decade) and global average time series for the period 1951–2010 for cold spell duration index (CSDI) and warm spell duration index (WSDI) in HadEX2. Missing data and significance criteria as in Figure 3. Global average time series are shown as anomalies relative to the 1961–1990 average (thin blue line); 21 point Gaussian filtered data (thick blue line) are also shown.

[28] Associated with the widespread warming trends, there is also a tendency toward shorter cold spell duration (Figure 5a) and, conversely, longer warm spell duration (Figure 5b) in most areas. These changes are significant for both indices in most of Eurasia. India stands out as having much stronger increasing trends in the warm spell duration index (WSDI) than most other regions. Maximum temperatures in India have increased by about  $1.1^{\circ}\text{C}$  since the beginning of the twentieth century with particularly large positive anomalies in the last couple of decades for both maximum and minimum temperatures [IMD, 2011]. Owing to the stipulation of the 1961–1990 base period, the region has experienced an excess of heatwave days since the mid-1990s by this definition [also see, e.g., Met Office, 2011], and this has inflated the trend in WSDI (see also section 5). Globally averaged, WSDI has increased by approximately 8 days since the middle of the twentieth century; however, most of this increase has occurred since 1980. Conversely,

the duration of cold spells has significantly decreased over large areas, by about 4 days since 1950 when considering the global average.

[29] On centennial time scales, since the beginning of the twentieth century, warming trends show mostly similar patterns to the trends estimated since the middle of last century. However, the trends are more pronounced over the 1951–2010 period when compared to the 1901–2010 period, particularly for the frequency of warm/cold days/nights (Figure 3). Also on the longer time scale we find significant warming in the percentile-based indices over most parts of the world with data coverage, except for daytime temperatures over the eastern U.S. and southern South America. Changes in the absolute values are less spatially coherent; however, regions with significant changes have the same sign of trend in both periods. Note, however, that most of the observed warming occurred since the mid-1970s, and therefore on the centennial time scale



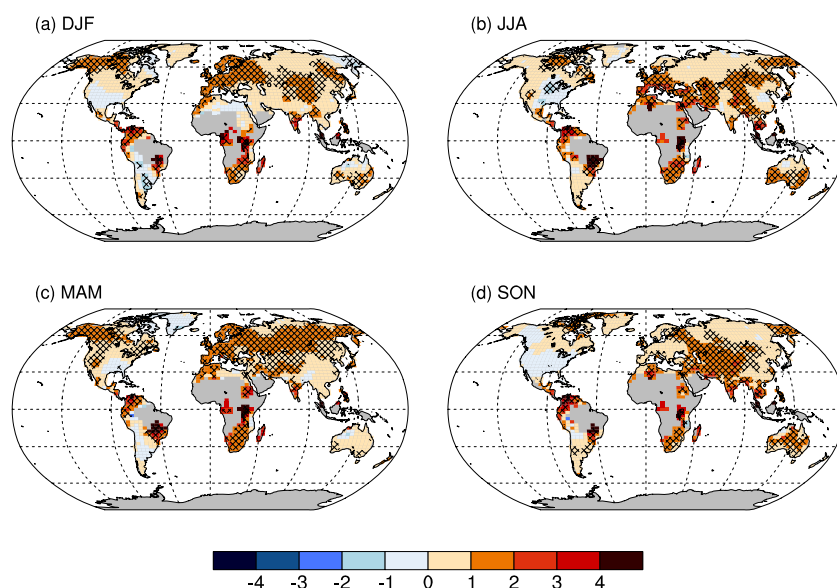


**Figure 6.** Trends (in days per decade) for seasonal series of warm days (TX90p) for the period 1951–2010 for (a) December–February, (b) June–August, (c) March–May, and (d) September–November. Trends were calculated using same criteria as in Figure 3.

most of the trend is due to the strong warming during the most recent decades.

#### 4.2. Trends in Seasonal Temperature Indices

[30] The warming trends related to the annual frequencies of warm/cool days/nights (Figure 3) can in general also be found throughout all seasons, however with differing magnitude and significance. The seasonal results presented here were calculated as seasonal averages of the monthly gridded

fields. The frequency of warm days (Figure 6), for example, shows a tendency toward stronger and more extended warming during winter (i.e., December–January–February (DJF) on the Northern Hemisphere and June–July–August (JJA) on the Southern Hemisphere) and the transition seasons than in summer, particularly at higher latitudes. For the two regions where local cooling trends were observed (compare Figure 3d), seasonal analysis shows that this cooling is most significant during the summer months,

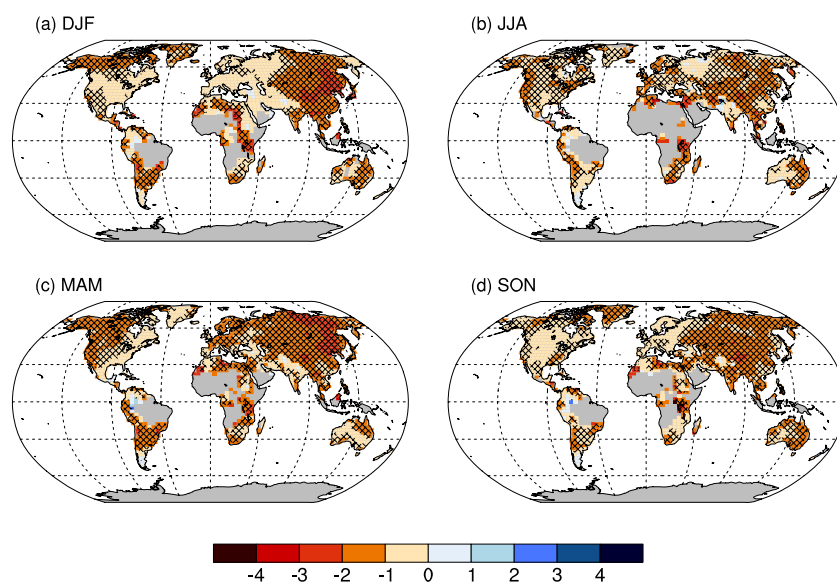
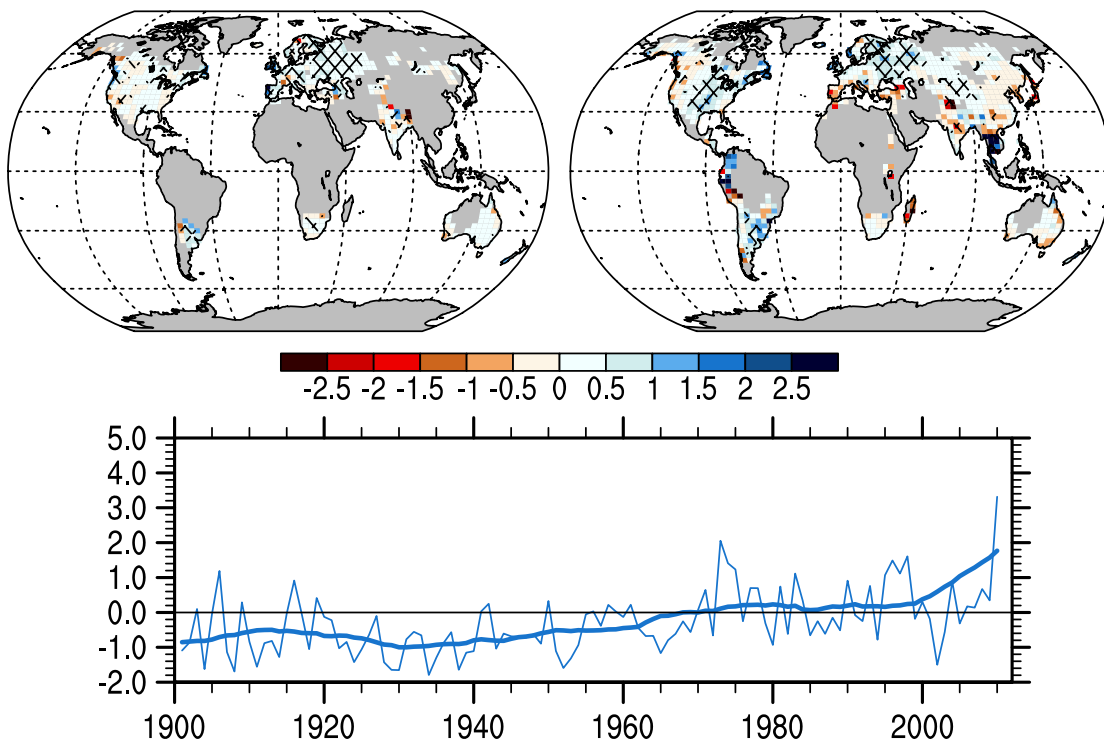


**Figure 7.** Trends (in days per decade) for seasonal series of cool nights (TN10p) for the period 1951–2010 for (a) December–February, (b) June–August, (c) March–May, and (d) September–November. Trends were calculated using same criteria as in Figure 3.

## (a) heavy precipitation days (R10mm)



## (b) contribution from very wet days (R95pTOT)

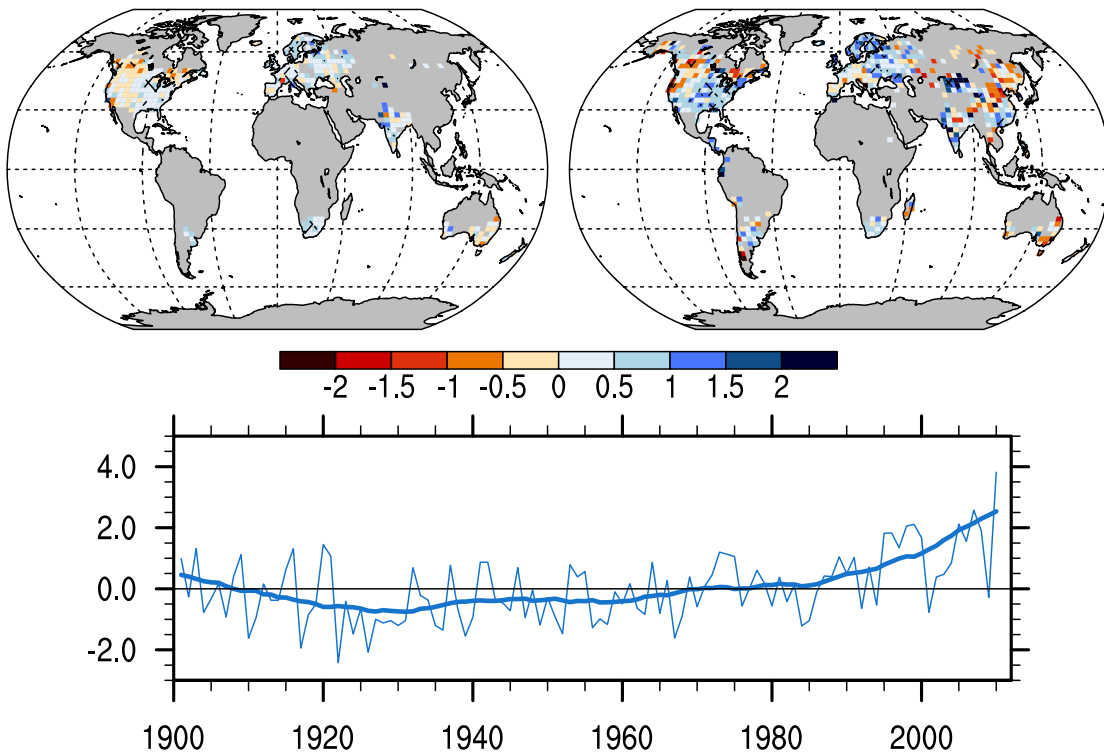
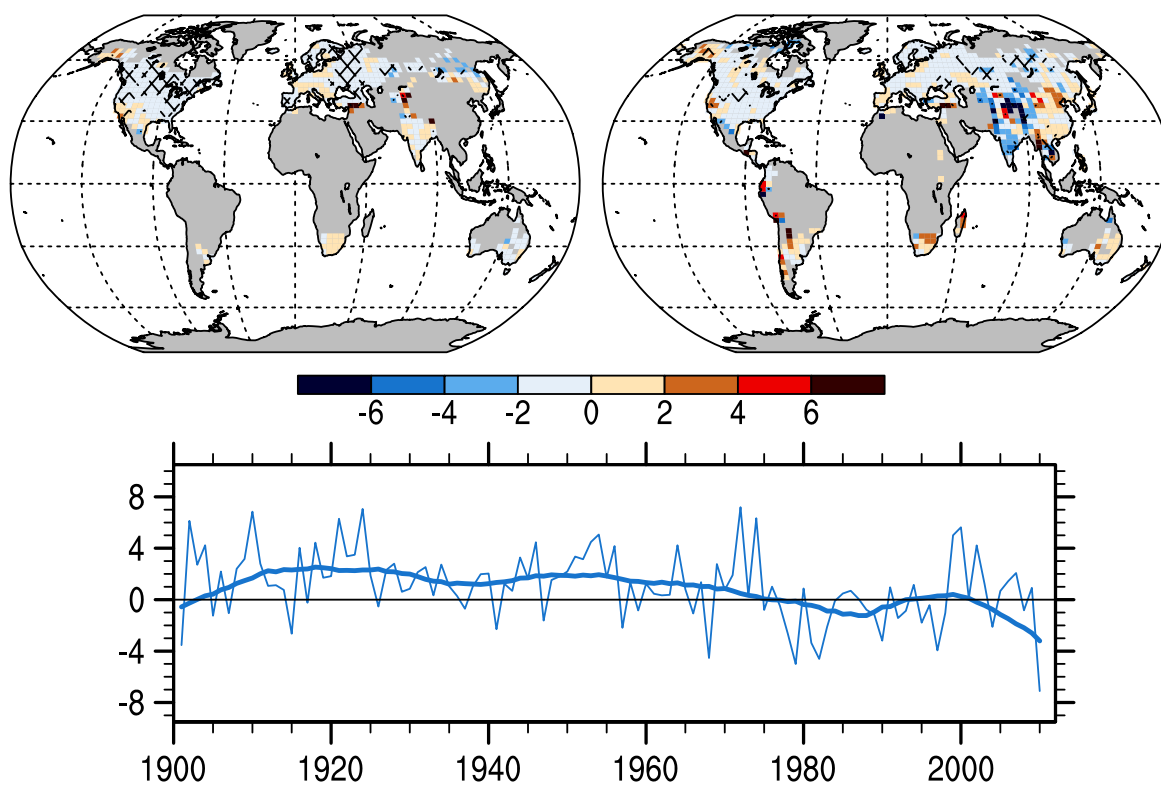


**Figure 8.** Decadal trends and global average time series for annual indices. (a) Number of heavy precipitation days (R10) in days, (b) contribution from very wet days (R95pTOT) in %, (c) consecutive dry days (CDD) in days, and (d) simple daily intensity index (SDII) in millimeters per day. Trend and time series calculations as described in Figure 3.

## (c) consecutive dry days (CDD)



## (d) simple daily intensity index (SDII)

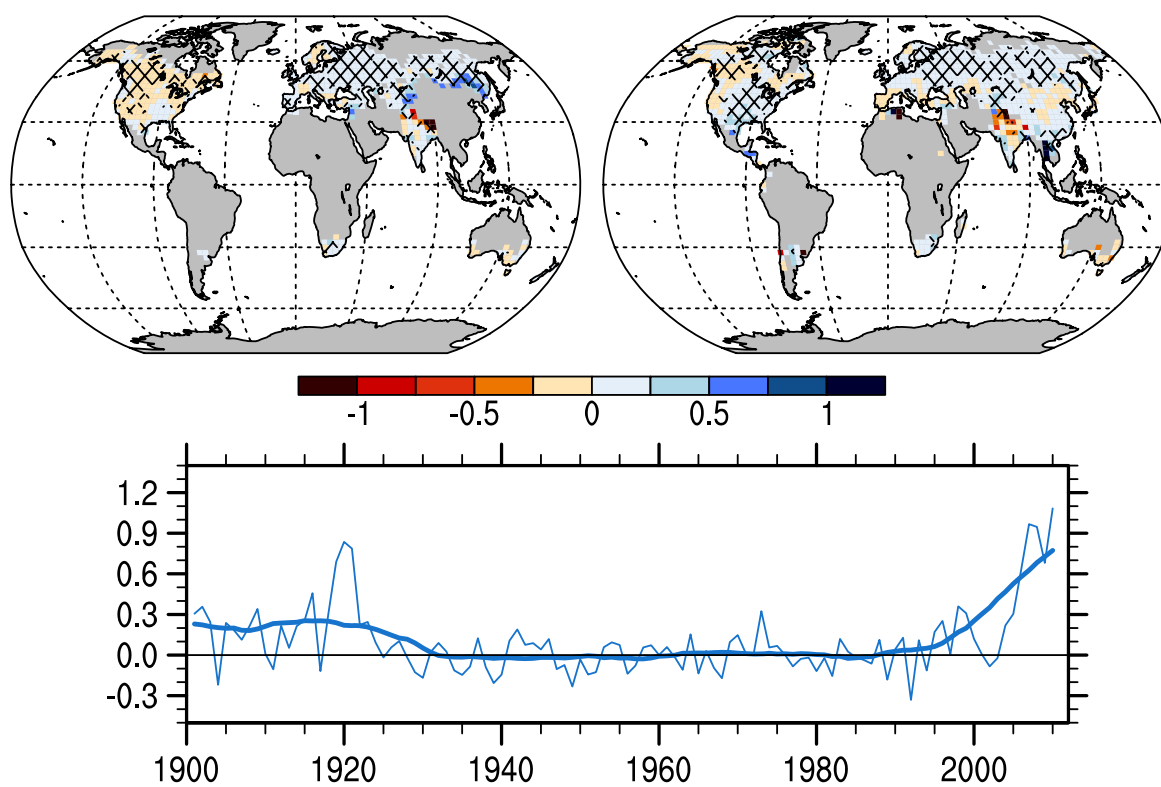
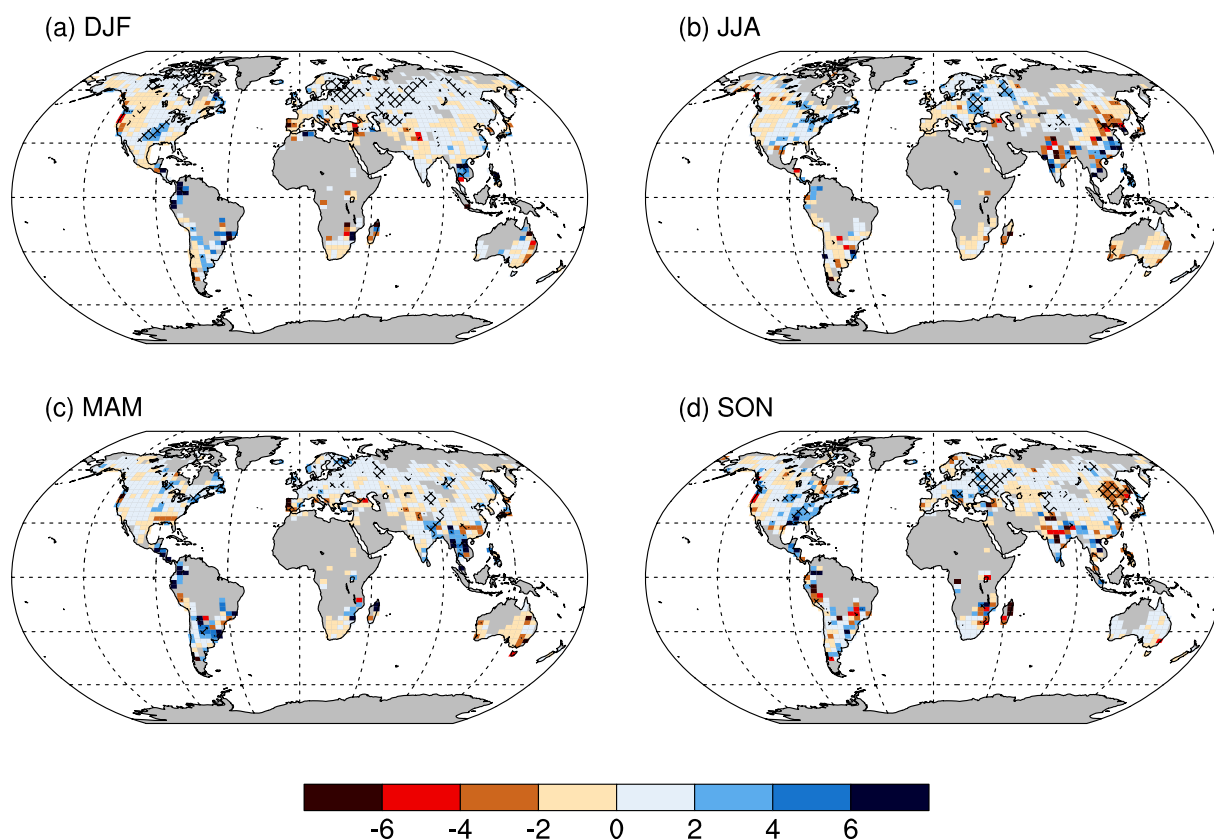


Figure 8. (Continued)



**Figure 9.** Trends (in mm/decade) for seasonal series of maximum consecutive 5 day precipitation (Rx5day) for the period 1951–2010 for (a) December–February, (b) June–August, (c) March–May, and (d) September–November. Trends were calculated using same criteria as in Figure 3.

**Table 3.** Land-based Grid Boxes Filled by Data Meeting the Data Completeness Criteria (See Text) for Each Index along with the Percentage of those Grid Boxes That Show Either a Significant Increase or Decrease at the 5% Level during the 1951–2010 Period

Index	Number of Land-based Grid Boxes	% Significant Increase	% Significant Decrease
TXx	1110	32.16	5.95
TNx	1056	63.73	3.22
TXn	1333	52.21	4.05
TNn	1336	70.36	3.14
TN10p	1398	0.36	96.92
TX10p	1400	0.36	84.00
TN90p	1587	98.61	0.00
TX90p	1437	76.55	1.25
DTR	1079	8.90	59.31
GSL	1250	41.36	5.36
ID	1496	3.07	39.44
FD	1278	3.05	67.37
SU	1271	46.66	6.61
TR	1032	48.74	4.36
WSDI	1182	69.63	0.59
CSDI	1003	3.19	68.89
Rx1day	420	21.90	7.14
Rx5day	438	23.97	8.22
SDII	880	46.48	8.64
R10	853	28.96	10.32
R20	568	28.87	9.15
CDD	832	5.77	21.15
CWD	435	18.39	11.03
R95p	561	30.66	5.88
R99p	420	25.00	4.05
PRCPTOT	986	41.28	9.84
ETR	1207	5.30	50.70
R95pTOT	561	23.89	4.99
R99pTOT	420	19.76	4.05



i.e., June–August for the “warming hole” in North America and December–February over South America, respectively.

[31] The frequency of cool nights also decreases consistently throughout all seasons (Figure 7). Particularly over Asia, this warming seems to be somewhat stronger during the cold months than during summer. On the contrary, Europe and South America show stronger warming during their respective summer months than in winter.

#### 4.3. Trends in Annual Precipitation Indices

[32] Although based on a larger number of stations (see Table 1), the gridded fields of the precipitation indices exhibit a less widespread spatial coverage than the temperature indices. This is a consequence of the lower correlation of the precipitation measures between neighboring stations (see section 3 and Figures 1b and 1d).

[33] The patterns of recent changes in precipitation indices appear spatially more heterogeneous than the consistent warming pattern seen in the temperature indices. Most of the precipitation indices show (partly significant) changes toward more intense precipitation over the eastern half of North America as well as over large parts of Eastern Europe, Asia, and South America. Areas with trends toward less frequent and intense precipitation are observed, e.g., around the Mediterranean, in Southeast Asia, and the northwestern part of North America. Such changes in extreme precipitation are found, for example, for the number of heavy precipitation days (R10mm, Figure 8a) and the contribution from very wet days (R95pTOT, Figure 8b). Globally averaged, both indices display upward trends during the past 60 years. Similar patterns of change are also found for the average intensity of daily precipitation (Figure 8d). All precipitation-based indices show larger areas with significant trends toward wetter conditions than areas with drying trends (Table 3).

[34] The number of consecutive dry days (CDD, Figure 8c), a measure for extremely dry conditions, also shows trends toward shorter duration of dry spells (i.e., fewer CDD) over larger parts of North America, Europe, and Southern Asia, whereas nonsignificant trends toward dryer conditions are found over East Asia, eastern Australia, South Africa, and portions of South America where sufficient data are available for trend calculations. Globally, no clear trend can be identified.

[35] As for the temperature indices, trends in the precipitation indices over the whole 1901–2010 period are largely similar in pattern to the trends since 1951 (where data are available); however, they are usually smaller in magnitude.

#### 4.4. Trends in Seasonal Precipitation Indices

[36] Only two of the precipitation indices, Rx1day and Rx5day, have data available for sub-annual timescales (see Table 1). We calculated the seasonal values of both indices as the seasonal maxima of the monthly gridded fields. Seasonal trends are generally comparable with annual trends (not shown). The annual maximum consecutive 5 day precipitation amount, for example, displays significant tendencies toward stronger extreme precipitation over eastern North America and large parts of Europe and Asia comparable with results shown in Figure 8. In these areas, the increase in extreme precipitation is visible across all seasons (Figure 9) but tends to be more significant during

winter and autumn (DJF and September–October–November (SON) in the Northern Hemisphere). Some tropical regions in South America and Southeast Asia also display a strong increase in extreme precipitation between 1951 and 2010 across the seasons, particularly during December to May. However, as spatial coverage is limited for tropical regions, a detailed investigation of this was not possible.

### 5. Discussion

[37] Our results support previous studies, including A2006, that have found a shift in the distribution of both maximum and minimum temperature extremes consistent with warming and that globally averaged minimum temperature extremes are warming faster than maximum temperature extremes. Recent studies have shown how the distributions of both daily and seasonal temperatures have significantly shifted toward higher temperature values since the middle of the twentieth century [Hansen *et al.*, 2012; Donat and Alexander, 2012]. This includes changes in the higher statistical moments of the distributions, having serious implications for climate impacts.

[38] The driving mechanisms related to the reported changes may vary between regions and time scales, but large-scale natural variability plays a role [e.g., Haylock *et al.*, 2006; Barrucand *et al.*, 2008; Scaife *et al.*, 2008; Alexander *et al.*, 2009; Caesar *et al.*, 2011; Renom *et al.*, 2011], as do changes in anthropogenic greenhouse gases [e.g., Kiktev *et al.*, 2003; Alexander and Arblaster, 2009; Min *et al.*, 2011] and land-use and land cover change [e.g., Avila *et al.*, 2012]. There is also some (generally seasonally dependent) covariability between temperature extremes and other atmospheric variables, such as precipitation, cloud cover, or the occurrence of storms [e.g., Robinson *et al.*, 2002; Portmann *et al.*, 2009]. Results presented here confirm, for example, that the “warming hole” as reflected by reduced maximum temperatures over eastern North America seems to be related to more intense precipitation in this region.

[39] This study also indicates that on the whole the globally averaged trends in HadEX2 temperature and precipitation indices compare very well with the trends in HadEX over the period when both datasets overlap and particularly when both datasets are masked with the same grid boxes and even though largely different input data have been used (Figure A1). Some minor differences in the time series of the global averages (mostly toward the end of the series), for example TNx or CDD, largely vanish when the HadEX2 fields are masked to grid boxes where HadEX has nonmissing data (dashed lines in Figure A1). This shows that differences between area-averaged time series from both data sets can primarily be explained by the different spatial coverage. Some larger differences during the last years of comparison after 2000, as seen, e.g., for TNn, TXn, R10mm, or SDII can be explained by a drop in grid box coverage in HadEX after 2000. The differences would largely vanish if we applied an even stricter data completeness criterion, requiring, e.g., 100% of data for grid cells to contribute to the global time series. The similarity in trends from both datasets, given the largely different input data, gives additional confidence to the robustness of the results.

[40] There are two exceptions, however, in that there are some differences in the warm spell (WSDI) and cold spell (CSDI) duration indices. For these two indices, there are some larger discrepancies between the new HadEX2 data set and HadEX, and this is related to inconsistencies in the calculation of these indices in HadEX. *Sillmann et al.* [2012] discuss how this is likely caused by the use of an earlier version of the RClimDex/FClimDex code to calculate indices for the U.S., which did not account for insufficient data precision (in part due to rounding to whole degrees Fahrenheit) in the data, leading to a bias in the temperature percentile exceedance rates estimated (this is discussed in *Zhang et al.* [2009]). Hence, caution should be applied to analysis of CSDI and WSDI in HadEX especially over the North American region, although other regions are fairly comparable. Owing to partly different spell duration calculation between the two datasets, even masking HadEX2 to grid boxes where HadEX had valid data (dashed blue line in Figure A1) does not minimize the differences for these indices. Indeed, the masked data are largely similar to the unmasked HadEX2 global WSDI and CSDI averages. In the new HadEX2 dataset, the indices were calculated using the same software for all input stations, and the gridded fields do not suffer from such inconsistencies. However, by definition these indices are statistically “volatile” in that they have a tendency to contain many zeros and have no warm spells defined for periods shorter than 6 days; thus, other heat wave metrics that are more statistically robust are being proposed to replace them [*Perkins et al.*, 2012]. Consequently, even in HadEX2 some caution is required in assessing results for the cold and warm spell duration indices. Larger differences between HadEX and HadEX2 are also obvious for growing season length (GSL), reflecting a problem with this index in the previous version of the data set. In HadEX, some stations with a continuous (365 day) growing season were assigned a growing season length of 0 days. This has been corrected in HadEX2. Another point of note is the large value of Rx1day that occurs in 1982 in HadEX but is not present in HadEX2. On inspection, this appears to be a result of particularly high and likely erroneous precipitation values in some U.S. stations in HadEX which do not appear in HadEX2. Since data in both datasets were obtained from a subset of GHCN-Daily for the U.S., we assume that values that appeared in an earlier version of GHCN-Daily have since been corrected.

[41] Several precipitation extremes are also related to snow or heavy precipitation on subdaily time scales. As we aim to produce an “as-global-as-possible” dataset, we rely on the ETCCDI climate indices, and these do not consider snow or subdaily precipitation. Given the limitations in coverage and availability already when using daily data, hourly precipitation data are even more confined such that at present a global observation-based dataset of subdaily extremes does not seem feasible. A more detailed investigation of seasonal precipitation extremes based on HadEX2 is also limited by the fact that the ETCCDI indices at present are calculated monthly for only two precipitation indices, Rx1day and Rx5day.

[42] While HadEX2 is a gridded dataset and therefore is likely to be used in future model evaluation studies, we add a cautionary note that care must be taken to distinguish between gridded products when evaluating extremes. In the

method employed here, our output is more closely representative of regularly spaced point locations. Climate model output and reanalysis products more typically represent the area average of a grid. While in the case of most temperature indices the two measures might be almost indistinguishable, for other indices such as annual maxima or minima or those derived from daily precipitation, these gridded metrics might represent quite different values [e.g., *Chen and Knutson*, 2008]. There is some debate as to whether it would be more appropriate to grid the daily data first and then calculate the indices as this might better reflect the measures that are returned by climate models or reanalyses. However, calculating indices in this way would likely have the effect of over-smoothing the extremes [*Hofstra et al.*, 2010]. In addition, it adds a level of structural uncertainty into the resulting data, the effects of which have yet to be tested in detail [e.g., *Donat et al.*, 2012a]. However, interpolation of daily data has been shown to reduce the intensity of extremes [*Haylock et al.*, 2008] and is argued to be more comparable with climate model data. We therefore recommend that these caveats are taken into account when using HadEX2 for model evaluation.

## 6. Conclusions

[43] We present a new global land-based gridded dataset of climate extremes indices. This dataset, HadEX2, is the outcome of major data collection efforts, and it substantially enhances a previous dataset (HadEX, A2006) by providing improved spatial coverage, updates for the most recent years up to 2010, and an extension back in time to the beginning of the twentieth century. The new dataset also solves some issues with regionally inconsistent calculations of indices in HadEX. The analysis of recent changes in climate extremes largely confirms the conclusions based on the previous dataset, hence generating increased confidence in the robustness of the presented trends. The main findings include widespread and significant warming trends related to temperature extremes indices, mostly stronger for indices based on daily minimum temperatures than for indices calculated from daily maximum temperatures. The changes in precipitation extremes are in general spatially more complex and mostly locally less significant. However, on a global scale, we find a tendency toward wetter conditions for most precipitation indices, i.e., the intensity, frequency, and duration of extreme precipitation is increasing on average.

[44] It should be noted that there are still large data gaps over regions such as Africa and northern South America, although international efforts are ongoing to try and fill in these gaps [e.g., *Skansi et al.*, 2012] and to provide a data monitoring capability for the ETCCDI indices [*Donat et al.*, 2012a]. At present though, the spatial distribution of stations is still insufficient to provide a truly global picture of changes in extremes, particularly for those extremes related to precipitation. It is hoped that efforts will continue to address the need for continuous data collection and that ideally all data would be shared with the international science community through a central data base (such as the GHCN-Daily dataset). Note that the data presented in this paper, both station-based (where permissible) and gridded indices, are available from [www.climdex.org](http://www.climdex.org).

## Appendix A

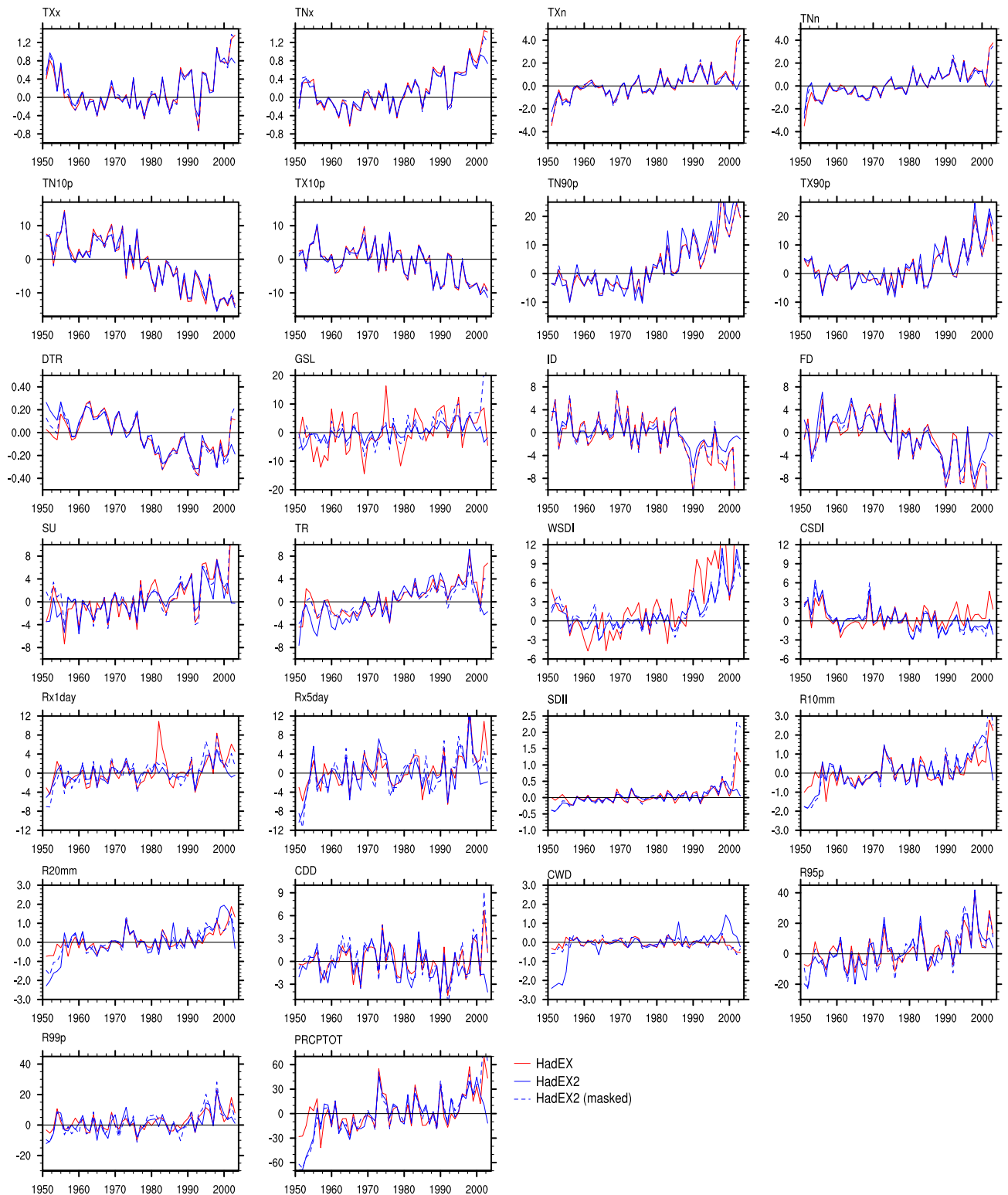


**Figure A1.** Global average time series of annual index values (anomalies relative to 1961–1990 mean values) for 26 of the Expert Team on Climate Change Detection and Indices (ETCCDI) core indices for HadEX2 (blue lines) in comparison to HadEX (red lines; A2006) over the 1951–2003 period (for which HadEX had data). For the calculation of global averages, only grid boxes with at least 90% of \ coverage are used, i.e., 48 years during 1951–2003. HadEX2 is also masked to grid boxes where HadEX had data (blue dashed lines) to show that most of the differences can be attributed to different spatial coverage. Units as indicated in Table 1.



[45] **Acknowledgments.** Donat, Alexander, and Yang are supported by Australian Research Council grants CE110001028 and LP100200690. Dunn, Willett, and Caesar were supported by the Joint DECC/Defra Met Office Hadley Centre Climate Programme (GA01101). Marengo, Renom, and Rusticucci are supported by European Community's Seventh Framework Programme (FP7/2007–2013) Grant Agreement N° 212492: CLARIS LPB-A Europe-South America Network for Climate Change Assessment and Impact Studies in La Plata Basin, Marengo also from the FAPESP Assessment of Impacts and Vulnerability to Climate Change in Brazil and strategies for Adaptation options project (Ref. 2008/581611) and Rusticucci also from CONICET PIP-0227. We acknowledge the Sudan Meteorological Authority (SMA) and National Meteorological and Hydrological Services from countries around the world for providing observational data. We also thank the three anonymous reviewers who helped to improve this manuscript.

## References

- Aguilar, E., et al. (2009), Changes in temperature and precipitation extremes in western central Africa, Guinea Conakry, and Zimbabwe, 1955–2006, *Journal of Geophysical Research-Atmospheres*, **114**, D02115, doi:10.1029/2008JD011010.
- Alexander, L. V., et al. (2006), Global observed changes in daily climate extremes of temperature and precipitation, *Journal of Geophysical Research-Atmospheres*, **111**, D05109, doi:10.1029/2005JD006290.
- Alexander, L. V., J. M. Arblaster (2009), Assessing trends in observed and modelled climate extremes over Australia in relation to future projections, *International Journal of Climatology*, **29**, 417–435 DOI:10.1002/joc.1730.
- Alexander, L. V., P. Uotila, and N. Nicholls (2009), Influence of sea surface temperature variability on global temperature and precipitation extremes, *Journal of Geophysical Research-Atmospheres*, **114**, D18116, doi:10.1029/2009JD012301.
- Avila, F. B., A. J. Pitman, M. G. Donat, L. V. Alexander, G. Abramowitz (2012), Climate model simulated changes in temperature extremes due to land cover change, *Journal of Geophysical Research-Atmospheres*, **117**, D04108, DOI: 10.1029/2011JD016382.
- Barrucand, M., M. Rusticucci, and W. Vargas (2008), Temperature extremes in the south of South America in relation to Atlantic Ocean surface temperature and Southern Hemisphere circulation, *Journal of Geophysical Research*, **113**, D20111, doi:10.1029/2007JD009026.
- Caesar, J., L. Alexander, and R. Vose (2006), Large-scale changes in observed daily maximum and minimum temperatures: Creation and analysis of a new gridded data set, *Journal of Geophysical Research-Atmospheres*, **111**, D05101, doi:10.1029/2005JD006280.
- Caesar, J., et al. (2011), Changes in temperature and precipitation extremes over the Indo-Pacific region from 1971 to 2005, *International Journal of Climatology*, **31**, 791–801, doi:10.1002/joc.2118.
- Chen, C.-T., and T. Knutson (2008), On the verification and comparison of extreme rainfall indices from climate models, *J. Climate*, **21**(7), 1605–1621, doi:10.1175/2007JCLI1494.1.
- Donat M. G., and L. V. Alexander (2012), The shifting probability distribution of global daytime and night-time temperatures, *Geophysical Research Letters*, **39**, L14707, 5 doi:10.1029/2012GL052459.
- Donat, M. G., I. Durre, H. Yang, L. V. Alexander, R. Vose, J. Caesar (2012a), Global land-based datasets for monitoring climatic extremes, *Bulletin of the American Meteorological Society*, in press.
- Donat, M. G., et al. (2012b), Changes of extreme temperature and precipitation in the Arab region: Long-term trends and variability related to ENSO and NAO, (submitted to *International Journal of Climatology*).
- Durre, I., M. J. Menne, B. E. Gleason, T. G. Houston, and R. S. Vose (2010), Comprehensive automated quality assurance of daily surface observations, *Journal of Applied Meteorology and Climatology*, **8**, 1615–1633.
- Frich, P., L. V. Alexander, P. Della-Marta, B. Gleason, M. Haylock, A. Klein Tank, T. Peterson (2002), Observed coherent changes in climatic extremes during the second half of the 20th century, *Climate Research*, **19**, 193–212.
- Hansen, J., M. Sato, and R. Ruedy, 2012, Perception of climate change, *Proc. Natl. Acad. Sci.*, **109**, 14726–14727, E2415–E2423, doi:10.1073/pnas.0808533106.
- Haylock, M. R., et al. (2006), Trends in total and extreme South American rainfall 1960–2000 and links with sea surface temperature, *Journal of Climate*, **19**, 1490–1512.
- Haylock, M. R., N. Hofstra, A. M. G. Klein Tank, E. J. Klok, P. D. Jones, and M. New, (2008), A European daily high-resolution gridded data set of surface temperature and precipitation, for 1950–2006, *Journal of Geophysical Research*, **113**, D20119, doi:10.1029/2008JD010201.
- Hofstra, N., M. New, and C. McSweeney, (2010), The influence of interpolation and station network density on the distributions and trends of climate variables in gridded daily data, *Climate Dynamics*, **35**(5), 841–858, doi:10.1007/s00382-009-0698-1.
- India Meteorological Department (IMD), (2011), Annual climate summary.
- Kendall, M. G. (1975) Rank Correlation Methods. Charles Griffin, London.
- Kiktev, D., D. Sexton, L. Alexander, C. Folland (2003), Comparison of modelled and observed trends in indicators of daily climate extremes, *Journal of Climate*, **16**(22), 3560–71.
- Klok, E. J. and A. M. G. Klein Tank (2009), Updated and extended European dataset of daily climate observations, *International Journal of Climatology*, **29**(8), 1182–1191 DOI: 10.1002/joc.1779.
- Kruger, A. C., and S. S. Sekele (2012), Trends in extreme temperature indices in South Africa, 1962–2009, (online first), *International Journal of Climatology* DOI:10.1002/joc.3455
- Griffiths, G. M., M. J. Salinger, and I. Leleu (2003), Trends in extreme daily rainfall across the South Pacific and relationships to the SPCZ, *International Journal of Climatology*, **23**, 847–869.
- Mekis, E. and L. A. Vincent (2011) An overview of the second generation adjusted daily precipitation dataset for trend analysis in Canada, *Atmosphere-Ocean*, **49**(2), 163–177.
- Menne, M. J., I. Durre, B. G. Gleason, T. G. Houston, and R. S. Vose (2012), An overview of the Global Historical Climatology Network-Daily database, *Journal of Atmospheric and Oceanic Technology*, **29**, 897–910
- Menne, M. J., and C. N. Williams Jr. (2005), Detection of undocumented change-points using multiple test statistics and composite reference series, *Journal of Climate*, **18**, 4271–4286, doi:10.1175/JCLI3524.1.
- Met Office, (2011), Climate: observations, projections and impacts, published by Met Office, available at <http://www.metoffice.gov.uk/climate-change/policy-relevant/obs-projections-impacts>.
- Min, S.-K., X. Zhang, F. W. Zwiers, and G. C. Hegerl (2011), Human contribution to more-intense precipitation extremes, *Nature*, **470**(7334), 378–381, doi:10.1038/nature09763.
- Morak, S., G. G. Hegerl, J. Kenyon (2011), Detectable regional changes in the number of warm nights, *Geophysical Research Letters*, **38**, L17703, doi:10.1029/2011GL048531.
- New, M. G., M. Hulme, and P. D. Jones (2000), Representing twentieth century space-time climate variability. Part II: Development of 1901–96 monthly grids of terrestrial surface climate, *Journal of Climate*, **13**, 2217–2238.
- Nicholls, N. and L. Alexander (2007), Has the climate become more variable or extreme? Progress 1992–2006, *Progress in Physical Geography*, **31**, 1–11.
- Oria, C. (2012), Tendencia Actual de los Indicadores Extremos de Cambio Climático en la Cuenca del río Mantaro, Technical Note of the Centro de Predicción Numérica/Dirección General de Meteorología Servicio Nacional de Meteorología e Hidrología, Perú.
- Perkins S. E., L. V. Alexander, J. Naim (2012), Increasing frequency, intensity and duration of observed global heat waves and warm spells, *Geophysical Research Letters*, **39**, L20714, doi:10.1029/2012GL053361.
- Peterson, T. C., and M. J. Manton (2008), Monitoring changes in climate extremes: A tale of international collaboration, *Bulletin of the American Meteorological Society*, **89**, 1266–1271. DOI:10.1175/2008BAMS2501.1.
- Peterson, T. C., X. B. Zhang, M. Brunet-India, and J. L. Vazquez-Aguirre (2008), Changes in North American extremes derived from daily weather data, *Journal of Geophysical Research-Atmospheres*, **113**(D7), D07113.
- Portmann, R. W., S. Solomon, and G. C. Hegerl (2009), Spatial and seasonal patterns in climate change, temperatures, and precipitation across the United States, *Proc. Nat. Acad. Sci.*, **106**, 7324–7329, doi:10.1073/pnas.0808533106.
- Renom M., M. Rusticucci, and M. Barreiro (2011), Multidecadal changes in the relationship between extreme temperature events in Uruguay and the general atmospheric circulation, *Climate Dynamics*, **37** (11–12), 2471–2480.
- Robinson, W. A., R. Ruedy, and J. E. Hansen (2002), General circulation model simulations of recent cooling in the east-central United States, *Journal of Geophysical Research*, **107**, no. D24, 4748, doi:10.1029/2001JD001577.
- Rusticucci, M. (2012), Observed and simulated variability of extreme temperature events over South America, *Atmospheric Research*, **106**, 1–17.
- Rusticucci, M., J. Marengo, O. Penalba, M. Renom (2010), An intercomparison of model-simulated extreme rainfall and temperature events during the last half of twentieth century. Part 1: Mean values and variability, *Climatic Change*, **98** (3), 493–508.
- Rusticucci, M. and M., Renom (2008), Variability and trends in indices of quality-controlled daily temperature extremes in Uruguay, *International Journal of Climatology*, **28**, 1083–1095, DOI: 10.1002/joc.1607.
- Salinger, M. J., and G. Griffiths (2001), Trends in annual New Zealand daily temperature and rainfall extremes, *International Journal of Climatology*, **21**, 1437–1452.



- Scaife, A. A., C. K. Folland, L. V. Alexander, A. Moberg, and J. R. Knight (2008), European climate extremes and the North Atlantic Oscillation, *Journal Climate*, *21*, 72–83.
- Sen, P. K. (1968), Estimates of the regression coefficient based on Kendall's Tau, *Journal of the American Statistical Association*, *63*, 1379–1389.
- Shepard, D. (1968), A two-dimensional interpolation function for irregularly spaced data, paper presented at 23rd National Conference, *Assoc. for Comput. Mach.*, New York.
- Sillmann, J., and E. Roekner (2008), Indices for extreme events in projections of anthropogenic climate change, *Climate Change*, *86*(1–2), 83–104.
- Sillmann et al. 2012. Climate extreme indices in the CMIP5 multi-model 1 ensemble. Part 1: Model evaluation in the present climate, *Journal of Geophysical Research*, in press, DOI: 10.1002/jgrd.50203.
- Skansi, M. M., et al. (2012), Warming and wetting signals emerging from an analysis of changes in climate extreme indices over South America, *Global and Planetary Change*, in press.
- Trewin, B. (2012), A daily homogenized temperature data set for Australia, (online first), *International Journal of Climatology*, DOI: 10.1002/joc.3530.
- Villarreal, C., B. Rosenblüth and P. Aceituno (2006) Climate change along the extratropical west coast of South America (Chile): Daily max/min temperatures. 8<sup>th</sup> ICSHMO conference, Foz de Iguazu, April 2006
- Vincent, L. A., et al. (2011), Observed trends in indices of daily and extreme temperature and precipitation for the countries of the western Indian Ocean, 1961–2008, *Journal of Geophysical Research*, *116*, D10108, doi:10.1029/2010JD015303.
- Vincent, L. A., X. L. Wang, E. J. Milewska, H. Wan, F. Yang, and V. Swail (2012). A second generation of homogenized Canadian monthly surface air temperature for climate trend analysis, *Journal of Geophysical Research*, *117*, D18110, doi:10.1029/2012JD017859.
- Zhai, P. M., and X. Pan (2003), Trends in temperature extremes during 1951–1999 in China, *Geophys. Res. Lett.*, *30*(17), 1913, doi:10.1029.
- Zhai, P., X. Zhang, H. Wan, and X. Pan (2005), Trends in total precipitation and frequency of daily precipitation extremes over China, *Journal of Climate*, *18*, 1096–1108.
- Zhang, X., L. Alexander, G. C. Hegerl, P. Jones, A. Klein Tank, T. C. Peterson, B. Trewin, and F. W. Zwiers (2011), Indices for monitoring changes in extremes based on daily temperature and precipitation data, *WIREs Climate Change*, *2*, 851–870, doi:10.1002/wcc.147.
- Zhang, X., G. Hegerl, F. Zwiers, and J. Kenyon (2005), Avoiding inhomogeneity in percentile-based indices of temperature extremes, *Journal of Climate*, *18*, 1641–1651.
- Zhang, X., F. W. Zwiers, G. Hegerl (2009), The influence of data precision on the calculation of temperature percentile indices, *International Journal of Climatology*, *29*, 321–327. DOI:10.1002/joc.1738.
- Zwiers, F. W., et al. (2012). Challenges in estimating and understanding recent changes in the frequency and intensity of extreme climate and weather events. In: *Climate Science for Serving Society: Research, Modelling and Prediction Priorities*. G. R. Asrar and J. W. Hurrell, Eds. Springer, in press.